

A More General Linear Projectile Problem

Nick Lorenzo

Lorenzo.Nick@gmail.com

November 5, 2024

Abstract

In a full 3D context, we study a projectile subject to linear drag, a non-uniform gravitational field, time-dependent wind, and parameterized atmospheric thinning. In this general context, we provide integral solutions, exact to $\mathcal{O}(\varepsilon)$, for the position and velocity of the projectile, where ε is a small perturbation parameter; in the special case of constant wind, we provide closed-form solutions, exact to $\mathcal{O}(\varepsilon)$. Under the constant-wind assumption, we provide closed-form solutions of $\mathcal{O}(1)$ for the time of tangency, times of flight, and extreme values of the radius achieved by the projectile. We provide physical interpretations throughout, including a physical interpretation of the branches W_0 and W_{-1} of the Lambert W function in the context of flight time. We also provide parameterized, error-controlled algorithms to compute trajectories, complete with a full Matlab implementation that we make freely available. We compare the results of our implementation to a general-purpose, stiff ODE solver.

Contents

1	Introduction	2
1.1	Generalizations investigated in this work	2
1.2	Contributions of this work	3
2	Development of the projectile-motion model	3
3	Transformation of the model to dimensionless form	5
4	Spatial expansion of the dimensionless model	7
5	Integral solutions for time-dependent wind	8
5.1	Zeroth-order closed-form solution for $b_{\text{eff}} = 0$ and time-dependent wind	8
5.2	First-order integral solution for $b_{\text{eff}} = 0$ and time-dependent wind	9
5.3	Two-term expansion for $b_{\text{eff}} = 0$ and time-dependent wind	10
5.4	Zeroth-order integral solution for $b_{\text{eff}} \neq 0$ and time-dependent wind	10
5.5	First-order integral solution for $b_{\text{eff}} \neq 0$ and time-dependent wind	11
5.6	Two-term expansion for $b_{\text{eff}} \neq 0$ and time-dependent wind	12
6	Closed-form solutions for constant wind	12
6.1	Zeroth-order closed-form solution for $b_{\text{eff}} = 0$ and constant wind	12
6.2	First-order closed-form solution for $b_{\text{eff}} = 0$ and constant wind	12
6.3	Two-term expansion for $b_{\text{eff}} = 0$ and constant wind	13
6.4	Zeroth-order closed-form solution for $b_{\text{eff}} \neq 0$ and constant wind	13
6.5	First-order closed-form solution for $b_{\text{eff}} \neq 0$ and constant wind	13
6.6	Two-term expansion for $b_{\text{eff}} \neq 0$ and constant wind	14
7	Solutions of the original projectile-motion model	14

7.1	Zeroth-order solutions of the original projectile-motion model	15
7.2	Expanded solutions of the original projectile-motion model	15
8	Model parameters and validity	15
8.1	Choosing the parameters r_c and t_c	15
8.1.1	Bounding r_c based on η	16
8.1.2	Bounding r_c based on ε	16
8.1.3	Bounding r_c based on the spatial expansion of f_{atm}	16
8.1.4	Defining r_c	16
8.1.5	Defining t_c	17
8.2	Temporal region of validity of the model and its solutions	17
9	Analysis of zeroth-order trajectories with constant wind	18
9.1	Time of tangency	18
9.1.1	General condition for the time of tangency	18
9.1.2	Zeroth-order time of tangency for $b_{\text{eff}} = 0$	19
9.1.3	Zeroth-order time of tangency for $b_{\text{eff}} \neq 0$ and constant wind	19
9.2	Flight time	20
9.2.1	General condition for the flight time	20
9.2.2	Zeroth-order flight time for $b_{\text{eff}} = 0$	20
9.2.3	Zeroth-order flight time for $b_{\text{eff}} \neq 0$ and constant wind	21
9.3	Extreme radii	22
9.3.1	Maximum radius for $b_{\text{eff}} = 0$	23
9.3.2	Extreme radius for $b_{\text{eff}} \neq 0$ and constant wind	23
9.4	A note on the consistency of our results	23
10	Some numerical considerations	24
10.1	Estimating the parameter b_{drag}	24
10.2	Small values of b_{eff}	24
10.3	Parameterized, error-controlled algorithms	24
11	Numerical results	25
11.1	Quantities of interest	26
11.2	Trajectory comparisons	26
11.3	Some observations	29
12	Conclusion	29
A	Selected calculations of the integrals I_0 and I_1	29
B	Expansions in orders of b_{eff}	31
B.1	Expanded positions and velocities	31
B.2	Expanded times of tangency and flight	32

1 Introduction

The linear projectile problem is a classic problem in classical mechanics, receiving an elementary treatment in texts such as [1, Sec. 2.2]. More advanced treatments of the problem can be found in works such as [2] and [3], which study the problem with constant wind.

1.1 Generalizations investigated in this work

In this paper, we generalize the typical approach to the linear projectile problem in several ways.

- (1) We include the effects of a non-uniform gravitational field.

- (2) We permit an arbitrary, vector-valued, time-dependent wind function in 3D space.
- (3) We permit a parameterized atmospheric thinning function.
- (4) We permit an arbitrary initial position in 3D space, on or above the surface of the Earth.
- (5) We study the flight time of the projectile with respect to an arbitrary final radius, on or above the surface of the Earth.
- (6) We study the extreme value of the radius achieved by the projectile, whether that extreme value is a maximum or a minimum.
- (7) We permit an initial velocity of arbitrary magnitude and direction in 3D space.

1.2 Contributions of this work

Under the above generalizations, we provide the following contributions to the literature.

- (1) We develop the full 3D, nonlinear, coupled, second-order system of ODEs modeling the problem (Section 2).
- (2) We provide physical interpretations of the ODEs of both $\mathcal{O}(1)$ and $\mathcal{O}(\varepsilon)$, where ε is a small perturbation parameter (Section 5).
- (3) We provide integral solutions exact to $\mathcal{O}(\varepsilon)$ for the position and velocity of the projectile (Section 5).
- (4) We provide, in the special case of constant wind, closed-form solutions of both $\mathcal{O}(1)$ and $\mathcal{O}(\varepsilon)$ for the position and velocity of the projectile (Section 6), and we present numerical evidence that our $\mathcal{O}(\varepsilon)$ solutions increase the accuracy of our $\mathcal{O}(1)$ solutions with respect to the original model (Section 11).
- (5) We provide an analysis of the validity of our approximations and solutions (Section 8).
- (6) We provide general $\mathcal{O}(1)$ conditions on the time of tangency, times of flight, and extreme values of the radius achieved by the projectile (Section 9).
- (7) We provide, in the special case of constant wind, closed-form solutions of $\mathcal{O}(1)$ for the time of tangency, times of flight, and extreme values of the radius achieved by the projectile, with physical interpretations (Section 9).
- (8) We provide a physical interpretation of the relevant branches of the Lambert W function in the context of flight time (Section 9.2.3).
- (9) We provide a parameterized method of controlling the error in our solutions (Section 10.3).
- (10) We provide a full numerical implementation of our solutions with parameterized error control in the constant-wind case, including code to reproduce all the data and figures we present (see [6]).

2 Development of the projectile-motion model

Consider a non-relativistic, point-like projectile subject only to the force of Earth's gravitational field, \vec{F}_{grav} , and to the force of air resistance, \vec{F}_{air} . The net force on the projectile may be written as

$$\vec{F}_{\text{net}} = \vec{F}_{\text{grav}} + \vec{F}_{\text{air}}. \quad (1)$$

Let m be the mass of the projectile, let $g \approx 9.81$ meters / second² be the acceleration of gravity at the surface of the Earth, let $R_E \approx 6.361 \times 10^6$ meters be the radius of the Earth (which we assume to be spherical and of uniform density), and let $\vec{z}(t)$ be the position of the projectile at time t , with the origin at the center of the Earth. Then we may write the force of gravity as

$$\vec{F}_{\text{grav}} = -\frac{mgR_E^2}{z^3}\vec{z}, \quad (2)$$

where $z(t) \equiv |\vec{z}(t)| \geq R_E$ is the distance from the projectile to the center of the Earth at time t .

We assume the force of air resistance to be well-approximated by

$$\vec{F}_{\text{air}} \sim \vec{F}_{\text{air}}^{\text{lin}}, \quad (3)$$

where

$$\vec{F}_{\text{air}}^{\text{lin}} = -f_{\text{atm}}(s)b_{\text{drag}}\vec{v}^{\text{rel}} \quad (4)$$

is the force of linear resistance, with linear drag coefficient $b_{\text{drag}} \geq 0$ at sea level. The function $f_{\text{atm}} : [0, \infty) \rightarrow [0, 1]$ is a dimensionless atmospheric thinning function with dimensionless argument $s : [0, \infty) \rightarrow [0, \infty)$ defined by

$$s(t) \equiv \frac{z(t) - R_E}{\ell}; \quad (5)$$

$f_{\text{atm}}(s(t))$ models the density of air at radius $z(t)$ relative to the density of air at radius R_E (sea level). Here, $\ell > 0$ is a characteristic length scale for the atmospheric thinning function f_{atm} (see Section 11.2 for an example of f_{atm} and ℓ). The quantity

$$\vec{v}^{\text{rel}} \equiv \frac{d\vec{z}}{dt} - \vec{v}^{\text{wind}} \quad (6)$$

is the relative velocity of the projectile through the air, with the motion of the air itself modeled by the vector-valued, time-dependent wind function \vec{v}^{wind} .

Applying Newton's second law¹ to the projectile subject to the net force (1), we find the projectile's motion to be modeled by the nonlinear, coupled, second-order system of ODEs given by

$$m \frac{d^2 \vec{z}}{dt^2} = -\frac{mgR_E^2}{z^3}\vec{z} - f_{\text{atm}}\left(\frac{z - R_E}{\ell}\right) \left[\frac{d\vec{z}}{dt} - \vec{v}^{\text{wind}} \right] b_{\text{drag}}, \quad (7)$$

with initial conditions

$$\vec{z}(t=0) = \vec{z}_0 \equiv R_0 \vec{\alpha}, \quad (8a)$$

$$\frac{d\vec{z}}{dt}(t=0) = v_0 \vec{\beta}. \quad (8b)$$

Here, $R_0 \equiv z(t=0) \geq R_E$ is the initial distance from the projectile to the center of the Earth, v_0 is the initial speed of the projectile, and $\vec{\alpha}$ and $\vec{\beta}$ are vectors given in Cartesian coordinates by

$$\vec{\alpha} \equiv (\sin(\theta_r) \cos(\phi_r), \sin(\theta_r) \sin(\phi_r), \cos(\theta_r)), \quad (9)$$

$$\vec{\beta} \equiv (\sin(\theta_v) \cos(\phi_v), \sin(\theta_v) \sin(\phi_v), \cos(\theta_v)) \llbracket v_0 \neq 0 \rrbracket, \quad (10)$$

where $\theta_r \in [0, \pi]$ is the inclination angle and $\phi_r \in [0, 2\pi)$ is the azimuthal angle of the initial position of the projectile, and where $\theta_v \in [0, \pi]$ is the inclination angle and $\phi_v \in [0, 2\pi)$ is the azimuthal angle of the initial velocity of the projectile. Here, the notation $\llbracket X \rrbracket$ is the Iverson bracket, evaluated as 1 if X is true and 0 otherwise.

¹Here we neglect the fact that the Earth is a non-inertial, rotating reference frame. This can be handled by relating our results to a time-dependent coordinate system, but we do not develop that model here.

3 Transformation of the model to dimensionless form

Define the relative position $\vec{r}(t)$ of the projectile by

$$\vec{r}(t) \equiv \vec{z}(t) - \vec{z}_0. \quad (11)$$

Let $0 < t_c$ be a characteristic time for the problem, let $0 < r_c$ be a characteristic length for the problem (each to be specified in Section 8.1), and define the characteristic speed and scalar acceleration

$$v_c \equiv \frac{r_c}{t_c}, \quad (12a)$$

$$a_c \equiv \frac{r_c}{t_c^2}. \quad (12b)$$

We then define the dimensionless time τ , relative position $\vec{\rho}$, and wind \vec{w} by

$$\tau \equiv \frac{1}{t_c} t, \quad (13a)$$

$$\vec{\rho}(\tau) \equiv \frac{1}{r_c} \vec{r}(t(\tau)), \quad (13b)$$

$$\vec{w}(\tau) \equiv \frac{1}{v_c} \vec{v}^{\text{wind}}(t(\tau)). \quad (13c)$$

Here, from the relationship (13a),

$$t(\tau) \equiv t_c \tau. \quad (14)$$

We find that

$$\frac{d}{dt} = \frac{1}{t_c} \frac{d}{d\tau}, \quad (15a)$$

$$\frac{d^n \vec{z}}{dt^n} = \frac{d^n \vec{r}}{dt^n}, \quad (15b)$$

$$\frac{d^n}{dt^n} \vec{r}(t(\tau)) = \frac{r_c}{t_c^n} \frac{d^n}{d\tau^n} \vec{\rho}(\tau). \quad (15c)$$

Now, assume r_c is defined in such a way that

$$r_c \ll R_0 \quad (16)$$

is satisfied, and define the small, dimensionless parameter

$$\varepsilon \equiv \frac{r_c}{R_0} \ll 1. \quad (17)$$

Also define

$$\rho \equiv |\vec{\rho}|, \quad (18a)$$

$$\eta \equiv 2\varepsilon(\vec{\alpha} \cdot \vec{\rho}) + \varepsilon^2 \rho^2, \quad (18b)$$

$$u \equiv 1 + \eta. \quad (18c)$$

Now,

$$z^k = |\vec{z}|^k \quad (19a)$$

$$= |\vec{z}_0 + \vec{r}|^k \quad (19b)$$

$$= [|\vec{z}_0|^2 + 2(\vec{z}_0 \cdot \vec{r}) + |\vec{r}|^2]^{k/2} \quad (19c)$$

$$= [R_0^2 + 2R_0(\vec{\alpha} \cdot \vec{r}) + |\vec{r}|^2]^{k/2} \quad (19d)$$

$$= \left[R_0^2 \left(1 + \frac{2}{R_0} (\vec{\alpha} \cdot \vec{r}) + \frac{1}{R_0^2} |\vec{r}|^2 \right) \right]^{k/2} \quad (19e)$$

$$= R_0^k \left[1 + \frac{2}{R_0} (\vec{\alpha} \cdot \vec{r}) + \frac{1}{R_0^2} |\vec{r}|^2 \right]^{k/2} \quad (19f)$$

$$= R_0^k \left[1 + 2 \frac{r_c}{R_0} (\vec{\alpha} \cdot \vec{\rho}) + \frac{r_c^2}{R_0^2} \rho^2 \right]^{k/2} \quad (19g)$$

$$= R_0^k [1 + 2\varepsilon (\vec{\alpha} \cdot \vec{\rho}) + \varepsilon^2 \rho^2]^{k/2} \quad (19h)$$

$$= R_0^k u^{k/2} \quad (19i)$$

$$= R_0^k (1 + \eta)^{k/2} \quad (19j)$$

$$= R_0^k \left[1 + \frac{1}{2} k \eta + \frac{1}{8} k(k-2) \eta^2 + \mathcal{O}(\eta^3) \right] \quad (19k)$$

$$= R_0^k \left[1 + k\varepsilon (\vec{\alpha} \cdot \vec{\rho}) + \frac{1}{2} k\varepsilon^2 \{ \rho^2 + (k-2)(\vec{\alpha} \cdot \vec{\rho})^2 \} + \mathcal{O}(\varepsilon^3) \right]. \quad (19l)$$

The accuracy of the expansion in powers of η depends on the value of η ; we later specify this accuracy by placing a bound on η . This leads to a bound for ε , and therefore for r_c (see Section 8.1). For now, we assume that $\eta \ll 1$.

We note that

$$s = \kappa(u^{1/2} - \Gamma), \quad (20)$$

where

$$\Gamma \equiv \frac{R_E}{R_0} \leq 1 \quad (21)$$

and

$$\kappa \equiv \frac{R_0}{\ell}. \quad (22)$$

With (21), (12) – (18), (19i), and (20) in mind, we find that the original model (7) becomes

$$ma_c \frac{d^2 \vec{\rho}}{d\tau^2} = - \frac{mg\Gamma^2}{R_0 u^{3/2}} (R_0 \vec{\alpha} + r_c \vec{\rho}) - f_{\text{atm}} \left(\kappa(u^{1/2} - \Gamma) \right) v_c b_{\text{drag}} \left[\frac{d\vec{\rho}}{d\tau} - \vec{w} \right], \quad (23)$$

which we rewrite more compactly as

$$\vec{\rho}'' = (\vec{\gamma} + \varepsilon \gamma \vec{\rho}) u^{-3/2} - f_{\text{atm}}(s) b(\vec{\rho}' - \vec{w}). \quad (24)$$

This is the general form of our dimensionless model, where

$$\gamma \equiv - \frac{g\Gamma^2}{a_c}, \quad (25a)$$

$$\vec{\gamma} \equiv \gamma \vec{\alpha}, \quad (25b)$$

$$b \equiv \frac{t_c}{m} b_{\text{drag}}. \quad (25c)$$

Physical interpretation In (25a), the factor Γ^2 adjusts the value of g to account for values of R_0 not equal to R_E , while division by the characteristic (scalar) acceleration a_c makes γ dimensionless; we therefore think of $|\gamma|$ as the dimensionless value of g we would find at a radius R_0 from the center of the Earth, and we think of $\vec{\gamma}$ as the corresponding dimensionless, vector-valued acceleration having fixed direction along the $\vec{\alpha}$ -axis defined by $\{x\vec{\alpha} \mid x \in \mathbb{R}\}$. The quantity b is the dimensionless linear drag coefficient.

We note that (24) is still an exact representation of the original model (7), as no approximations have yet been made. Define the dimensionless initial speed and dimensionless initial velocity

$$\delta \equiv \frac{v_0}{v_c}, \quad (26a)$$

$$\vec{\delta} \equiv \delta \vec{\beta}. \quad (26b)$$

Then we also find the dimensionless version of the initial conditions (8) to be given by

$$\vec{\rho}(0) = \vec{0}, \quad (27a)$$

$$\vec{\rho}'(0) = \vec{\delta}. \quad (27b)$$

We note that a solution $\vec{\rho}$ to the IVP defined by (24) and (27) necessarily depends on the choice of atmospheric thinning function f_{atm} , its parameter ℓ , the choice of r_c defining ε , the choice of t_c relating t and τ , the value of the air resistance parameter b_{drag} , and the choice of wind function \vec{v}^{wind} .

4 Spatial expansion of the dimensionless model

Defining $s_0 \equiv s(t=0)$ and using (19), we find that

$$s - s_0 = \frac{z - R_0}{\ell} \quad (28a)$$

$$= \frac{1}{\ell} [r_c(\vec{\alpha} \cdot \vec{\rho}) + \mathcal{O}(\varepsilon)] \quad (28b)$$

$$= \kappa \varepsilon (\vec{\alpha} \cdot \vec{\rho}) + \mathcal{O}(\varepsilon^2). \quad (28c)$$

We assume that $f_{\text{atm}}(s)$ may be written as

$$f_{\text{atm}}(s) = f_{\text{atm}}(s_0) + (s - s_0)f'_{\text{atm}}(s_0) + \frac{1}{2}(s - s_0)^2 f''_{\text{atm}}(s_0) + \dots \quad (29a)$$

$$= f_{\text{atm}}(s_0) + \kappa \varepsilon (\vec{\alpha} \cdot \vec{\rho}) f'_{\text{atm}}(s_0) + \mathcal{O}(\varepsilon^2). \quad (29b)$$

We note that the atmospheric expansion (29) is a good approximation when $\kappa \varepsilon (\vec{\alpha} \cdot \vec{\rho}) \ll 1$. Due to our later bounding of ρ by ρ_{max} (see Section 8.1), this is guaranteed if

$$\kappa \varepsilon \rho_{\text{max}} = \frac{r_c \rho_{\text{max}}}{\ell} \ll 1; \quad (30)$$

we assume that r_c has been defined such that (30) holds (see Section 8.1). Using the expansions (19l) and (29), we find that the dimensionless model (24) becomes

$$\vec{\rho}'' = (\vec{\gamma} + \varepsilon \gamma \vec{\rho}) u^{-3/2} - f_{\text{atm}}(s) b(\vec{\rho}' - \vec{w}) \quad (31a)$$

$$= (\vec{\gamma} + \varepsilon \gamma \vec{\rho}) [1 - 3\varepsilon(\vec{\alpha} \cdot \vec{\rho}) + \mathcal{O}(\varepsilon^2)] - [f_{\text{atm}}(s_0) + \kappa \varepsilon (\vec{\alpha} \cdot \vec{\rho}) f'_{\text{atm}}(s_0) + \mathcal{O}(\varepsilon^2)] b(\vec{\rho}' - \vec{w}) \quad (31b)$$

$$= \vec{\gamma} + \varepsilon \gamma \vec{\rho} - 3\vec{\gamma} \varepsilon (\vec{\alpha} \cdot \vec{\rho}) - f_{\text{atm}}(s_0) b(\vec{\rho}' - \vec{w}) - \kappa \varepsilon (\vec{\alpha} \cdot \vec{\rho}) f'_{\text{atm}}(s_0) b(\vec{\rho}' - \vec{w}) + \mathcal{O}(\varepsilon^2) \quad (31c)$$

$$= \vec{\gamma} - f_{\text{atm}}(s_0) b(\vec{\rho}' - \vec{w}) + \varepsilon [\gamma \vec{\rho} - 3\vec{\gamma}(\vec{\alpha} \cdot \vec{\rho}) - \kappa(\vec{\alpha} \cdot \vec{\rho}) f'_{\text{atm}}(s_0) b(\vec{\rho}' - \vec{w})] + \mathcal{O}(\varepsilon^2) \quad (31d)$$

$$= \vec{\gamma} - b_{\text{eff}}(\vec{\rho}' - \vec{w}) + \varepsilon [\gamma \vec{\rho} - 3\vec{\gamma}(\vec{\alpha} \cdot \vec{\rho}) - b'_{\text{eff}}(\vec{\alpha} \cdot \vec{\rho})(\vec{\rho}' - \vec{w})] + \mathcal{O}(\varepsilon^2), \quad (31e)$$

where

$$b_{\text{eff}} \equiv f_{\text{atm}}(s_0) b, \quad (32a)$$

$$b'_{\text{eff}} \equiv \kappa f'_{\text{atm}}(s_0) b. \quad (32b)$$

We think of b_{eff} as the effective dimensionless linear drag coefficient at radius R_0 , and we think of b'_{eff} as the effective rate of change of b_{eff} there.

We assume that a solution to the spatially expanded model (31) with initial conditions (27) exists and has the form

$$\vec{\rho} = \vec{\rho}_0 + \varepsilon \vec{\rho}_1 + \mathcal{O}(\varepsilon^2). \quad (33)$$

Substituting (33) into (31), we find that

$$\vec{\rho}_0'' + \varepsilon \vec{\rho}_1'' + \mathcal{O}(\varepsilon^2) = \vec{\gamma} - b_{\text{eff}}(\vec{\rho}_0' - \vec{w}) + \varepsilon[\gamma \vec{\rho}_0 - 3\vec{\gamma}(\vec{\alpha} \cdot \vec{\rho}_0) - b'_{\text{eff}}(\vec{\alpha} \cdot \vec{\rho}_0)(\vec{\rho}_0' - \vec{w}) - b_{\text{eff}}\vec{\rho}_1'] + \mathcal{O}(\varepsilon^2), \quad (34)$$

where we have collected the RHS in powers of ε .

The initial conditions (27) can similarly be written in powers of ε , resulting in the initial conditions

$$\mathcal{O}(1) : \quad \vec{\rho}_0(0) = \vec{0}, \quad (35a)$$

$$\vec{\rho}_0'(0) = \vec{\delta}, \quad (35b)$$

$$\mathcal{O}(\varepsilon) : \quad \vec{\rho}_1(0) = \vec{0}, \quad (35c)$$

$$\vec{\rho}_1'(0) = \vec{0}. \quad (35d)$$

The result (34) is an expansion of the dimensionless model (24) in terms of dimensionless functions $\vec{\rho}_j$, each corresponding to a power j of the small, dimensionless parameter ε . We note that the coupled, nonlinear term \vec{F}_{grav} appearing in the original model (7) is now approximated by de-coupled, linear functions in (34), providing a significant simplification. Similar comments apply to the atmospheric thinning function f_{atm} .

5 Integral solutions for time-dependent wind

We split our study of the IVP given by (34) and (35) into two cases.²

(1) The first case is defined by the condition

$$b_{\text{eff}} = 0. \quad (\mathbf{bz})$$

The case **(bz)** is that of quasi-negligible air resistance: b_{eff} is negligible, due to a very small value of b or to a very small value of $f_{\text{atm}}(s_0)$ (or to a very small product of those factors), but b'_{eff} has no such restriction, as the air resistance may be changing in a non-negligible way.

(2) The second case is defined by the condition

$$b_{\text{eff}} \neq 0 \quad (\mathbf{bnz})$$

and accounts for cases of non-negligible air resistance.

5.1 Zeroth-order closed-form solution for $b_{\text{eff}} = 0$ and time-dependent wind

To find the zeroth-order solution $\vec{\rho}_0(\tau; (\mathbf{bz}))$ of the Ansatz (33), we equate the $\mathcal{O}(1)$ terms of the ODE (34) after enforcing the condition **(bz)** and include the $\mathcal{O}(1)$ initial conditions given by (35) to find the IVP

$$\mathcal{O}(1) : \quad \vec{\rho}_0''(\tau; (\mathbf{bz})) = \vec{\gamma}, \quad (36a)$$

$$\vec{\rho}_0'(0; (\mathbf{bz})) = \vec{\delta}, \quad (36b)$$

$$\vec{\rho}_0(0; (\mathbf{bz})) = \vec{0}. \quad (36c)$$

²We split up the cases $b_{\text{eff}} = 0$ and $b_{\text{eff}} \neq 0$ because, for each j , in the j^{th} -order problem, b_{eff} multiplies $\vec{\rho}_j'$; this causes the quantity $1/b_{\text{eff}}$ to appear, which is singular when $b_{\text{eff}} = 0$. There is an additional, third regime where $0 < b_{\text{eff}} \ll 1$ that becomes important in numerical implementations; see Section 10.2 and Appendix B. We also note that the solutions for the case $b_{\text{eff}} = 0$ can be found from Taylor expansions of the solutions for the case $b_{\text{eff}} \neq 0$ (because the singularities mentioned above are removable), but we find it instructive to treat the two cases separately.

Since we have enforced the condition (\mathbf{bz}) on the ODE (34) before seeking our solution, we've included that condition as a special argument of the solution, after the semicolon. We then integrate (36) to write the zeroth-order solutions, for $0 \leq \tau \leq \tau_*$, as

$$\vec{\rho}_0'(\tau; (\mathbf{bz})) = \vec{\delta} + \vec{\gamma}\tau, \quad (37a)$$

$$\vec{\rho}_0(\tau; (\mathbf{bz})) = \tau(\vec{\delta} + \frac{1}{2}\vec{\gamma}\tau), \quad (37b)$$

where τ_* , defined in (90), ensures the quality of our approximations. Hence the scalar components of the vector-valued, zeroth-order solution $\vec{\rho}_0$ are completely de-coupled from one another.

Physical interpretation The solution $\vec{\rho}_0$ is the dimensionless, scaled, translated, approximate solution to the physical problem modeled by (7), neglecting the effects of air resistance (and therefore wind) and assuming the force of gravity to have constant strength $|\gamma|$ and fixed direction $-\vec{\alpha}$ (pointing radially inward from the initial position of the projectile).

5.2 First-order integral solution for $b_{\text{eff}} = 0$ and time-dependent wind

Equating the $\mathcal{O}(\varepsilon)$ terms of the ODE (34) and the $\mathcal{O}(\varepsilon)$ initial conditions given by (35), we find the IVP

$$\mathcal{O}(\varepsilon) : \quad \vec{\rho}_1''(\tau; (\mathbf{bz})) = \vec{q}(\tau; (\mathbf{bz})), \quad (38a)$$

$$\vec{\rho}_1'(0; (\mathbf{bz})) = \vec{0}, \quad (38b)$$

$$\vec{\rho}_1(0; (\mathbf{bz})) = \vec{0}, \quad (38c)$$

where

$$\vec{q}(\tau; (\mathbf{bz})) \equiv \gamma\vec{\rho}_0(\tau; (\mathbf{bz})) - 3[\vec{\alpha} \cdot \vec{\rho}_0(\tau; (\mathbf{bz}))]\vec{\gamma} - b'_{\text{eff}}[\vec{\alpha} \cdot \vec{\rho}_0(\tau; (\mathbf{bz}))][\vec{\rho}_0'(\tau; (\mathbf{bz})) - \vec{w}(\tau)]. \quad (39)$$

Since the RHS of the ODE (38a) contains only the known, zeroth-order solution $\vec{\rho}_0$, the scalar components of the unknown first-order solution $\vec{\rho}_1$ defined in (33) have been effectively de-coupled.

Defining³

$$\sigma \equiv \vec{\alpha} \cdot \vec{\beta} \quad (40)$$

and using the fact that $|\vec{\alpha}| = 1$, we find from (37) that

$$\vec{\alpha} \cdot \vec{\rho}_0(\tau; (\mathbf{bz})) = \tau(\delta\sigma + \frac{1}{2}\gamma\tau). \quad (41)$$

We may then write the ODE (38a) more explicitly as

$$\vec{\rho}_1''(\tau; (\mathbf{bz})) = \vec{c}_1\tau + \vec{c}_2\tau^2 + \vec{c}_3\tau^3 + c_4(\tau)\vec{w}(\tau), \quad (42)$$

where

$$\vec{c}_1 \equiv \gamma\vec{\delta} - 3\delta\sigma\vec{\gamma} - b'_{\text{eff}}\delta\sigma\vec{\delta}, \quad (43a)$$

$$\vec{c}_2 \equiv -(\gamma\vec{\gamma} + b'_{\text{eff}}\delta\sigma\vec{\gamma} + \frac{1}{2}b'_{\text{eff}}\gamma\vec{\delta}), \quad (43b)$$

$$\vec{c}_3 \equiv -\frac{1}{2}b'_{\text{eff}}\gamma\vec{\gamma}, \quad (43c)$$

$$c_4(\tau) \equiv b'_{\text{eff}}\tau(\delta\sigma + \frac{1}{2}\gamma\tau). \quad (43d)$$

Integrating (42) and using the initial conditions of (38), we find, for $0 \leq \tau \leq \tau_*$, that

$$\vec{\rho}_1'(\tau; (\mathbf{bz})) = \frac{1}{2}\vec{c}_1\tau^2 + \frac{1}{3}\vec{c}_2\tau^3 + \frac{1}{4}\vec{c}_3\tau^4 + \int_0^\tau c_4(\tau')\vec{w}(\tau')d\tau'. \quad (44a)$$

³We note the following physical significance of σ when $v_0 \neq 0$: $\sigma = 1$ indicates radially outward initial motion along the $\vec{\alpha}$ -axis; $\sigma > 0$ indicates initial motion with both an outward and a tangential component; $\sigma = 0$ indicates initial motion perpendicular to the $\vec{\alpha}$ -axis (that is, initial motion tangential to the surface of the Earth); $\sigma < 0$ indicates initial motion with both an inward and a tangential component; $\sigma = -1$ indicates radially inward initial motion along the $\vec{\alpha}$ -axis.

Integrating (44a), we find that the solution to the $\mathcal{O}(\varepsilon)$ IVP (38) can be written, for $0 \leq \tau \leq \tau_*$, as

$$\vec{\rho}_1(\tau; (\mathbf{bz})) = \frac{1}{6}\vec{c}_1\tau^3 + \frac{1}{12}\vec{c}_2\tau^4 + \frac{1}{20}\vec{c}_3\tau^5 + \int_0^\tau \int_0^{\tau'} c_4(\tau'')\vec{w}(\tau'')d\tau''d\tau'. \quad (44b)$$

Physical interpretation To physically interpret the ODE (38a), we define

$$\vec{\rho}_0^\parallel \equiv (\vec{\alpha} \cdot \vec{\rho}_0)\vec{\alpha} \quad (45)$$

to be the component of $\vec{\rho}_0$ parallel to the $\vec{\alpha}$ -axis, and we define

$$\vec{\rho}_0^\perp \equiv \vec{\rho}_0 - \vec{\rho}_0^\parallel \quad (46)$$

to be the component of $\vec{\rho}_0$ perpendicular to the $\vec{\alpha}$ -axis. We then write the ODE (38a) as

$$\vec{\rho}_1'' = 2|\gamma|\vec{\rho}_0^\parallel - |\gamma|\vec{\rho}_0^\perp - b'_{\text{eff}}(\vec{\alpha} \cdot \vec{\rho}_0)(\vec{\rho}_0' - \vec{w}). \quad (47)$$

We interpret the first two terms of the RHS of (47) to be a first correction to the $\mathcal{O}(1)$ dimensionless gravitational acceleration $\vec{\gamma}$ appearing on the RHS of (36a). The first term in the correction, $2|\gamma|\vec{\rho}_0^\parallel$, is a radial correction; it nudges the projectile along the $\vec{\alpha}$ -axis a little farther from its initial position, in whichever direction along the $\vec{\alpha}$ -axis it was already moving (inward or outward); this is a first correction to the $\mathcal{O}(1)$ approximation that the gravitational force has constant *magnitude*. The second term in the correction, $-|\gamma|\vec{\rho}_0^\perp$, is a correction in the plane perpendicular to the $\vec{\alpha}$ -axis; it dampens the motion of the projectile in this plane, serving as a first correction to the $\mathcal{O}(1)$ approximation that the gravitational force has constant *direction*.

The final term on the RHS of (47), $-b'_{\text{eff}}(\vec{\alpha} \cdot \vec{\rho}_0)(\vec{\rho}_0' - \vec{w})$, is a first-order correction to the zeroth-order approximation of constant atmospheric density. We note that this correction contains a factor of $\vec{\alpha} \cdot \vec{\rho}_0$ because f_{atm} is a function of the radial distance of the projectile from the center of the Earth.

5.3 Two-term expansion for $b_{\text{eff}} = 0$ and time-dependent wind

We define the two-term expansion $\vec{\rho}_{\text{expanded}}$ to be the result of collecting and scaling the solutions given by (37) and (44b), with the expanded velocity defined similarly: for $0 \leq \tau \leq \tau_*$,

$$\vec{\rho}_{\text{expanded}}(\tau; (\mathbf{bz})) \equiv \vec{\rho}_0(\tau; (\mathbf{bz})) + \varepsilon\vec{\rho}_1(\tau; (\mathbf{bz})), \quad (48a)$$

$$\vec{\rho}'_{\text{expanded}}(\tau; (\mathbf{bz})) \equiv \vec{\rho}'_0(\tau; (\mathbf{bz})) + \varepsilon\vec{\rho}'_1(\tau; (\mathbf{bz})). \quad (48b)$$

The two-term expansion $\vec{\rho}_{\text{expanded}}$ is the dimensionless, scaled, translated, approximate solution to the problem modeled by (31) in the case of quasi-negligible air resistance (\mathbf{bz}), with the force of gravity spatially linearized about the initial position \vec{z}_0 of (8).

5.4 Zeroth-order integral solution for $b_{\text{eff}} \neq 0$ and time-dependent wind

To find the zeroth-order solution $\vec{\rho}_0(\tau; (\mathbf{bnz}))$ of the Ansatz (33), we equate the $\mathcal{O}(1)$ terms of the ODE (34) after enforcing the condition (\mathbf{bnz}) and include the $\mathcal{O}(1)$ initial conditions given by (35) to find the IVP

$$\mathcal{O}(1): \quad \vec{\rho}_0''(\tau; (\mathbf{bnz})) = \vec{\gamma} - b_{\text{eff}}[\vec{\rho}_0'(\tau; (\mathbf{bnz})) - \vec{w}(\tau)], \quad (49a)$$

$$\vec{\rho}_0'(0; (\mathbf{bnz})) = \vec{\delta}, \quad (49b)$$

$$\vec{\rho}_0(0; (\mathbf{bnz})) = \vec{0}. \quad (49c)$$

Define

$$\tau_d \equiv \frac{1}{b_{\text{eff}}} \quad (50)$$

to be the time scale over which the initial velocity of the projectile decays. Then the solution to the IVP (49) is

$$\vec{\rho}_0(\tau; (\mathbf{bnz})) \equiv \tau_d \left[\vec{\gamma}\tau + (\vec{\delta} - \tau_d \vec{\gamma})(1 - e^{-\tau/\tau_d}) \right] + b_{\text{eff}} I_1[\vec{w}](\tau), \quad (51a)$$

with velocity

$$\vec{\rho}_0'(\tau; (\mathbf{bnz})) \equiv \vec{\delta} e^{-\tau/\tau_d} + \tau_d \vec{\gamma}(1 - e^{-\tau/\tau_d}) + b_{\text{eff}} e^{-\tau/\tau_d} I_0[\vec{w}](\tau), \quad (51b)$$

where, for $n \in \{0, 1\}$ and for h a function of a single variable, we define

$$I_n[h](\tau) \equiv \llbracket n = 0 \rrbracket \int_0^\tau e^{\tau'/\tau_d} h(\tau') d\tau' + \llbracket n = 1 \rrbracket \int_0^\tau e^{-\tau'/\tau_d} I_0[h](\tau') d\tau'. \quad (52)$$

In the event that h is vector-valued, we apply I_n component-wise.

Physical interpretation The ODE (49a) is a direct approximation of the original model (7) in dimensionless form, with the simplifying assumptions of a constant gravitational force and constant atmospheric thinning factor.

5.5 First-order integral solution for $b_{\text{eff}} \neq 0$ and time-dependent wind

Equating the $\mathcal{O}(\varepsilon)$ terms of the ODE (34) and the $\mathcal{O}(\varepsilon)$ initial conditions given by (35), we find the IVP

$$\mathcal{O}(\varepsilon) : \quad \vec{\rho}_1''(\tau; (\mathbf{bnz})) = \vec{q}(\tau; (\mathbf{bnz})) - b_{\text{eff}} \vec{\rho}_1'(\tau; (\mathbf{bnz})), \quad (53a)$$

$$\vec{\rho}_1'(0; (\mathbf{bnz})) = \vec{0}, \quad (53b)$$

$$\vec{\rho}_1(0; (\mathbf{bnz})) = \vec{0}, \quad (53c)$$

where

$$\vec{q}(\tau; (\mathbf{bnz})) \equiv \gamma \vec{\rho}_0(\tau; (\mathbf{bnz})) - 3[\vec{\alpha} \cdot \vec{\rho}_0(\tau; (\mathbf{bnz}))]\vec{\gamma} - b'_{\text{eff}}[\vec{\alpha} \cdot \vec{\rho}_0(\tau; (\mathbf{bnz}))][\vec{\rho}_0'(\tau; (\mathbf{bnz})) - \vec{w}(\tau)]. \quad (54)$$

The solution to this IVP is

$$\vec{\rho}_1(\tau; (\mathbf{bnz})) = I_1[x \mapsto \vec{q}(x; (\mathbf{bnz}))](\tau), \quad (55a)$$

with velocity

$$\vec{\rho}_1'(\tau; (\mathbf{bnz})) = e^{-\tau/\tau_d} I_0[x \mapsto \vec{q}(x; (\mathbf{bnz}))](\tau). \quad (55b)$$

We calculate

$$\begin{aligned} I_n[x \mapsto \vec{q}(x; (\mathbf{bnz}))](\tau) &= \gamma I_n[x \mapsto \vec{\rho}_0(x; (\mathbf{bnz}))](\tau) - 3[\vec{\alpha} \cdot I_n[x \mapsto \vec{\rho}_0(x; (\mathbf{bnz}))](\tau)]\vec{\gamma} \\ &\quad - b'_{\text{eff}} I_n[x \mapsto [\vec{\alpha} \cdot \vec{\rho}_0(x; (\mathbf{bnz}))]\vec{\rho}_0'(x; (\mathbf{bnz}))](\tau) \\ &\quad + b'_{\text{eff}} I_n[x \mapsto [\vec{\alpha} \cdot \vec{\rho}_0(x; (\mathbf{bnz}))]\vec{w}(x)](\tau), \end{aligned} \quad (56)$$

$$\begin{aligned} I_n[x \mapsto \vec{\rho}_0(x; (\mathbf{bnz}))](\tau) &= \tau_d(\vec{\delta} - \tau_d \vec{\gamma}) I_n[x \mapsto 1](\tau) + \tau_d \vec{\gamma} I_n[x \mapsto x](\tau) \\ &\quad - \tau_d(\vec{\delta} - \tau_d \vec{\gamma}) I_n[x \mapsto e^{-x/\tau_d}](\tau) + b_{\text{eff}} I_n[x \mapsto I_1[\vec{w}](x)](\tau), \end{aligned} \quad (57)$$

and

$$\begin{aligned} I_n[x \mapsto [\vec{\alpha} \cdot \vec{\rho}_0(x; (\mathbf{bnz}))]\vec{\rho}_0'(x; (\mathbf{bnz}))](\tau) \\ = I_n[x \mapsto \vec{\Omega}(x; (\mathbf{bnz}))](\tau) + \tau_d^2(\delta\sigma - \tau_d\gamma)\vec{\gamma} I_n[x \mapsto 1](\tau) + \tau_d^2\gamma\vec{\gamma} I_n[x \mapsto x](\tau) \end{aligned} \quad (58)$$

$$\begin{aligned}
& + \tau_d(\delta\sigma - \tau_d\gamma)(\vec{\delta} - 2\tau_d\vec{\gamma})I_n[x \mapsto e^{-x/\tau_d}](\tau) + \tau_d\gamma(\vec{\delta} - \tau_d\vec{\gamma})I_n[x \mapsto xe^{-x/\tau_d}](\tau) \\
& - \tau_d(\delta\sigma - \tau_d\gamma)(\vec{\delta} - \tau_d\vec{\gamma})I_n[x \mapsto e^{-2x/\tau_d}](\tau),
\end{aligned}$$

where

$$\begin{aligned}
\vec{\Omega}(\tau; (\mathbf{bnz})) & \equiv b_{\text{eff}}I_1[\vec{\alpha} \cdot \vec{w}](\tau)[\tau_d\vec{\gamma} + (\vec{\delta} - \tau_d\vec{\gamma})e^{-\tau/\tau_d} + b_{\text{eff}}e^{-\tau/\tau_d}I_0[\vec{w}](\tau)] \\
& + e^{-\tau/\tau_d}I_0[\vec{w}](\tau)[\gamma\tau + (\delta\sigma - \tau_d\gamma)(1 - e^{-\tau/\tau_d}) + b_{\text{eff}}^2I_1[\vec{\alpha} \cdot \vec{w}](\tau)],
\end{aligned} \tag{59}$$

with selected integrals I_n provided in Appendix A. The results above and in Appendix A, combined with linearity, provide integral representations of the solutions (55) in terms of the wind function \vec{w} .

Physical interpretation To physically interpret the ODE (53a), we first note that $\vec{q}(\tau; (\mathbf{bnz}))$ can be understood in the same way as $\vec{q}(\tau; (\mathbf{bz}))$. The remaining term, $-b_{\text{eff}}\vec{\rho}_1'(\tau; (\mathbf{bnz}))$, is the $\mathcal{O}(\varepsilon)$ force of linear air resistance, taking into account the Ansatz (33); it contains no wind term because the wind is assumed to be of $\mathcal{O}(1)$.

5.6 Two-term expansion for $b_{\text{eff}} \neq 0$ and time-dependent wind

We define the two-term expansion $\vec{\rho}_{\text{expanded}}$ to be the result of collecting and scaling the solutions given by (51a) and (55a), with the expanded velocity $\vec{\rho}_{\text{expanded}}'$ defined similarly: for $0 \leq \tau \leq \tau_*$,

$$\vec{\rho}_{\text{expanded}}(\tau; (\mathbf{bnz})) \equiv \vec{\rho}_0(\tau; (\mathbf{bnz})) + \varepsilon\vec{\rho}_1(\tau; (\mathbf{bnz})), \tag{60a}$$

$$\vec{\rho}_{\text{expanded}}'(\tau; (\mathbf{bnz})) \equiv \vec{\rho}_0'(\tau; (\mathbf{bnz})) + \varepsilon\vec{\rho}_1'(\tau; (\mathbf{bnz})). \tag{60b}$$

The two-term expansion $\vec{\rho}_{\text{expanded}}$ is the dimensionless, scaled, translated, approximate solution to the problem modeled by (31), in the case of non-negligible air resistance (\mathbf{bnz}), with the force of gravity spatially linearized about the initial position \vec{z}_0 of (8).

6 Closed-form solutions for constant wind

We write the special argument for this section as (\mathbf{cw}) , given by the condition

$$\vec{w}(\tau) \equiv \vec{w}_0 \exists \text{ fixed } \vec{w}_0 \in \mathbb{R}^3. \tag{cw}$$

6.1 Zeroth-order closed-form solution for $b_{\text{eff}} = 0$ and constant wind

The solutions (37) are independent of wind and therefore unaffected by the condition (\mathbf{cw}) ; we find that

$$\vec{\rho}_0(\tau; (\mathbf{bz}), (\mathbf{cw})) = \vec{\rho}_0(\tau; (\mathbf{bz})), \tag{61a}$$

$$\vec{\rho}_0'(\tau; (\mathbf{bz}), (\mathbf{cw})) = \vec{\rho}_0'(\tau; (\mathbf{bz})), \tag{61b}$$

both valid for $0 \leq \tau \leq \tau_*$.

6.2 First-order closed-form solution for $b_{\text{eff}} = 0$ and constant wind

Evaluating the solutions (44) using the condition (\mathbf{cw}) , we find that

$$\vec{\rho}_1'(\tau; (\mathbf{bz}), (\mathbf{cw})) = \frac{1}{2}\vec{c}_1\tau^2 + \frac{1}{3}\vec{c}_2\tau^3 + \frac{1}{4}\vec{c}_3\tau^4 + b_{\text{eff}}'\vec{w}_0\left(\frac{1}{2}\delta\sigma\tau^2 + \frac{1}{6}\gamma\tau^3\right), \tag{62a}$$

$$\vec{\rho}_1(\tau; (\mathbf{bz}), (\mathbf{cw})) = \frac{1}{6}\vec{c}_1\tau^3 + \frac{1}{12}\vec{c}_2\tau^4 + \frac{1}{20}\vec{c}_3\tau^5 + b_{\text{eff}}'\vec{w}_0\left(\frac{1}{6}\delta\sigma\tau^3 + \frac{1}{24}\gamma\tau^4\right), \tag{62b}$$

both valid for $0 \leq \tau \leq \tau_*$.

6.3 Two-term expansion for $b_{\text{eff}} = 0$ and constant wind

We define the two-term expansion $\vec{\rho}_{\text{expanded}}$ to be the result of collecting and scaling the solutions given by (61) and (62), with the expanded velocity defined similarly: for $0 \leq \tau \leq \tau_*$,

$$\vec{\rho}_{\text{expanded}}(\tau; (\mathbf{bz}), (\mathbf{cw})) \equiv \vec{\rho}_0(\tau; (\mathbf{bz}), (\mathbf{cw})) + \varepsilon \vec{\rho}_1(\tau; (\mathbf{bz}), (\mathbf{cw})), \quad (63a)$$

$$\vec{\rho}'_{\text{expanded}}(\tau; (\mathbf{bz}), (\mathbf{cw})) \equiv \vec{\rho}'_0(\tau; (\mathbf{bz}), (\mathbf{cw})) + \varepsilon \vec{\rho}'_1(\tau; (\mathbf{bz}), (\mathbf{cw})). \quad (63b)$$

The two-term expansion $\vec{\rho}_{\text{expanded}}$ is the dimensionless, scaled, translated, approximate solution to the problem modeled by (31) in the case of quasi-negligible air resistance and constant wind, with the force of gravity spatially linearized about the initial position \vec{z}_0 of (8).

6.4 Zeroth-order closed-form solution for $b_{\text{eff}} \neq 0$ and constant wind

Evaluating the solutions (51) using the condition (\mathbf{cw}) , we find that

$$\vec{\rho}_0(\tau; (\mathbf{bnz}), (\mathbf{cw})) = \vec{C}\tau + \tau_d \vec{D}(1 - e^{-\tau/\tau_d}), \quad (64a)$$

$$\vec{\rho}'_0(\tau; (\mathbf{bnz}), (\mathbf{cw})) = \vec{C} + e^{-\tau/\tau_d} \vec{D}, \quad (64b)$$

where

$$\vec{C} \equiv \vec{w}_0 + \tau_d \vec{\gamma}, \quad (65a)$$

$$\vec{D} \equiv \vec{\delta} - \vec{C}. \quad (65b)$$

6.5 First-order closed-form solution for $b_{\text{eff}} \neq 0$ and constant wind

Evaluating the solutions (55) using the condition (\mathbf{cw}) , we find that

$$\vec{\rho}_1(\tau; (\mathbf{bnz}), (\mathbf{cw})) = I_1[x \mapsto \vec{q}(x; (\mathbf{bnz}), (\mathbf{cw}))](\tau), \quad (66a)$$

$$\vec{\rho}'_1(\tau; (\mathbf{bnz}), (\mathbf{cw})) = e^{-\tau/\tau_d} I_0[x \mapsto \vec{q}(x; (\mathbf{bnz}), (\mathbf{cw}))](\tau), \quad (66b)$$

where

$$\begin{aligned} \vec{q}(\tau; (\mathbf{bnz}), (\mathbf{cw})) &\equiv \gamma \vec{\rho}_0(\tau; (\mathbf{bnz}), (\mathbf{cw})) - 3[\vec{\alpha} \cdot \vec{\rho}_0(\tau; (\mathbf{bnz}), (\mathbf{cw}))]\vec{\gamma} \\ &\quad - b'_{\text{eff}}[\vec{\alpha} \cdot \vec{\rho}_0(\tau; (\mathbf{bnz}), (\mathbf{cw}))][\vec{\rho}'_0(\tau; (\mathbf{bnz}), (\mathbf{cw})) - \vec{w}_0]. \end{aligned} \quad (67)$$

We calculate

$$\begin{aligned} I_n[x \mapsto \vec{q}(x; (\mathbf{bnz}), (\mathbf{cw}))](\tau) &= \gamma I_n[x \mapsto \vec{\rho}_0(x; (\mathbf{bnz}), (\mathbf{cw}))](\tau) \\ &\quad - 3[\vec{\alpha} \cdot I_n[x \mapsto \vec{\rho}_0(x; (\mathbf{bnz}), (\mathbf{cw}))](\tau)]\vec{\gamma} \\ &\quad - b'_{\text{eff}} I_n[x \mapsto [\vec{\alpha} \cdot \vec{\rho}_0(x; (\mathbf{bnz}), (\mathbf{cw}))]\vec{\rho}'_0(x; (\mathbf{bnz}), (\mathbf{cw}))](\tau) \\ &\quad + b'_{\text{eff}} I_n[x \mapsto [\vec{\alpha} \cdot \vec{\rho}_0(x; (\mathbf{bnz}), (\mathbf{cw}))]\vec{w}_0](\tau), \end{aligned} \quad (68)$$

$$I_n[x \mapsto [\vec{\alpha} \cdot \vec{\rho}_0(x; (\mathbf{bnz}), (\mathbf{cw}))]\vec{w}_0](\tau) = I_n[x \mapsto \tau_d(\vec{\alpha} \cdot \vec{D})\vec{w}_0 + (\vec{\alpha} \cdot \vec{C})\vec{w}_0 x - \tau_d(\vec{\alpha} \cdot \vec{D})\vec{w}_0 e^{-x/\tau_d}](\tau) \quad (69a)$$

$$\begin{aligned} &= \tau_d(\vec{\alpha} \cdot \vec{D})\vec{w}_0 I_n[x \mapsto 1](\tau) + (\vec{\alpha} \cdot \vec{C})\vec{w}_0 I_n[x \mapsto x](\tau) \\ &\quad - \tau_d(\vec{\alpha} \cdot \vec{D})\vec{w}_0 I_n[x \mapsto e^{-x/\tau_d}](\tau), \end{aligned} \quad (69b)$$

$$\begin{aligned} I_n[x \mapsto \vec{\rho}_0(x; (\mathbf{bnz}), (\mathbf{cw}))](\tau) &= \tau_d(\vec{\delta} - \tau_d \vec{\gamma}) I_n[x \mapsto 1](\tau) + \tau_d \vec{\gamma} I_n[x \mapsto x](\tau) \\ &\quad - \tau_d(\vec{\delta} - \tau_d \vec{\gamma}) I_n[x \mapsto e^{-x/\tau_d}](\tau) + b_{\text{eff}} I_n[x \mapsto I_1[y \mapsto \vec{w}_0](x)](\tau), \end{aligned} \quad (70)$$

$$I_n[x \mapsto I_1[y \mapsto \vec{w}_0](x)](\tau) = \vec{w}_0 I_n[x \mapsto I_1[y \mapsto 1](x)](\tau) \quad (71a)$$

$$= \vec{w}_0[-\tau_d^2 I_n[x \mapsto 1](\tau) + \tau_d I_n[x \mapsto x](\tau) + \tau_d^2 I_n[x \mapsto e^{-x/\tau_d}](\tau)], \quad (71b)$$

and

$$\begin{aligned} & I_n[x \mapsto [\vec{\alpha} \cdot \vec{\rho}_0(x; (\mathbf{bnz}), (\mathbf{cw}))]\vec{\rho}_0'(x; (\mathbf{bnz}), (\mathbf{cw}))](\tau) \\ &= I_n[x \mapsto \vec{\Omega}(x; (\mathbf{bnz}), (\mathbf{cw}))](\tau) + \tau_d^2(\delta\sigma - \tau_d\gamma)\vec{\gamma} I_n[x \mapsto 1](\tau) + \tau_d^2\gamma\vec{\gamma} I_n[x \mapsto x](\tau) \\ &+ \tau_d(\delta\sigma - \tau_d\gamma)(\vec{\delta} - 2\tau_d\vec{\gamma}) I_n[x \mapsto e^{-x/\tau_d}](\tau) + \tau_d\gamma(\vec{\delta} - \tau_d\vec{\gamma}) I_n[x \mapsto xe^{-x/\tau_d}](\tau) \\ &- \tau_d(\delta\sigma - \tau_d\gamma)(\vec{\delta} - \tau_d\vec{\gamma}) I_n[x \mapsto e^{-2x/\tau_d}](\tau), \end{aligned} \quad (72)$$

where

$$\begin{aligned} \vec{\Omega}(\tau; (\mathbf{bnz}), (\mathbf{cw})) &\equiv \tau_d[(\vec{\alpha} \cdot \vec{D})\vec{w}_0 - (\vec{\alpha} \cdot \vec{w}_0)\vec{C}] + [(\vec{\alpha} \cdot \vec{w}_0)\vec{C} + (\vec{\alpha} \cdot \vec{C})\vec{w}_0]\tau \\ &+ \tau_d[(\vec{\alpha} \cdot \vec{w}_0)\vec{C} - (\vec{\alpha} \cdot \vec{w}_0)\vec{D} - 2\vec{w}_0(\vec{\alpha} \cdot \vec{D})]e^{-\tau/\tau_d} + [(\vec{\alpha} \cdot \vec{w}_0)\vec{D} - (\vec{\alpha} \cdot \vec{C})\vec{w}_0]\tau e^{-\tau/\tau_d} \\ &+ \tau_d[(\vec{\alpha} \cdot \vec{w}_0)\vec{D} + (\vec{\alpha} \cdot \vec{D})\vec{w}_0]e^{-2\tau/\tau_d} \end{aligned} \quad (73)$$

and

$$\begin{aligned} I_n[x \mapsto \vec{\Omega}(x; (\mathbf{bnz}), (\mathbf{cw}))](\tau) &= \tau_d[(\vec{\alpha} \cdot \vec{D})\vec{w}_0 - (\vec{\alpha} \cdot \vec{w}_0)\vec{C}] I_n[x \mapsto 1](\tau) \\ &+ [(\vec{\alpha} \cdot \vec{w}_0)\vec{C} + (\vec{\alpha} \cdot \vec{C})\vec{w}_0] I_n[x \mapsto x](\tau) \\ &+ \tau_d[(\vec{\alpha} \cdot \vec{w}_0)\vec{C} - (\vec{\alpha} \cdot \vec{w}_0)\vec{D} - 2\vec{w}_0(\vec{\alpha} \cdot \vec{D})] I_n[x \mapsto e^{-x/\tau_d}](\tau) \\ &+ [(\vec{\alpha} \cdot \vec{w}_0)\vec{D} - (\vec{\alpha} \cdot \vec{C})\vec{w}_0] I_n[x \mapsto xe^{-x/\tau_d}](\tau) \\ &+ \tau_d[(\vec{\alpha} \cdot \vec{w}_0)\vec{D} + (\vec{\alpha} \cdot \vec{D})\vec{w}_0] I_n[x \mapsto e^{-2x/\tau_d}](\tau). \end{aligned} \quad (74)$$

The results of this section, together with linearity and the calculations of the integrals

$$I_n[x \mapsto \{1, x, e^{-x/\tau_d}, xe^{-x/\tau_d}, e^{-2x/\tau_d}\}](\tau)$$

found in Appendix A, provide a closed-form representation of the solutions (66).

6.6 Two-term expansion for $b_{\text{eff}} \neq 0$ and constant wind

We define the two-term expansion $\vec{\rho}_{\text{expanded}}$ to be the result of collecting and scaling the solutions given by (64a) and (66a), with the expanded velocity $\vec{\rho}'_{\text{expanded}}$ defined similarly: for $0 \leq \tau \leq \tau_*$,

$$\vec{\rho}_{\text{expanded}}(\tau; (\mathbf{bnz}), (\mathbf{cw})) \equiv \vec{\rho}_0(\tau; (\mathbf{bnz}), (\mathbf{cw})) + \varepsilon \vec{\rho}_1(\tau; (\mathbf{bnz}), (\mathbf{cw})), \quad (75a)$$

$$\vec{\rho}'_{\text{expanded}}(\tau; (\mathbf{bnz}), (\mathbf{cw})) \equiv \vec{\rho}'_0(\tau; (\mathbf{bnz}), (\mathbf{cw})) + \varepsilon \vec{\rho}'_1(\tau; (\mathbf{bnz}), (\mathbf{cw})). \quad (75b)$$

The two-term expansion $\vec{\rho}_{\text{expanded}}$ is the dimensionless, scaled, translated, approximate solution to the problem modeled by (31), in the case of non-negligible air resistance (\mathbf{bnz}) and constant wind (\mathbf{cw}), with the force of gravity spatially linearized about the initial position \vec{z}_0 of (8).

7 Solutions of the original projectile-motion model

In Sections 5 and 6 we provided various solutions to the dimensionless version of our problem, as introduced in Sections 3 and 4. We now discuss the transformations of these dimensionless solutions back to the original time and distance scales, producing solutions of the original model (7) with initial conditions (8).

7.1 Zeroth-order solutions of the original projectile-motion model

Using the definition (11) and scaling equations (13), we find that each zeroth-order position (and its zeroth-order velocity) – and approximate solution of the original, physically motivated system (7) with initial conditions (8) – can be written, for $0 \leq t \leq t_c \tau_\star$, in the form

$$\vec{z}_{\text{order } 0}(t; (\dots)) \equiv \vec{z}_0 + r_c \vec{\rho}_0 \left(\tau = \frac{t}{t_c}; (\dots) \right), \quad (76a)$$

$$\vec{z}'_{\text{order } 0}(t; (\dots)) \equiv v_c \vec{\rho}'_0 \left(\tau = \frac{t}{t_c}; (\dots) \right), \quad (76b)$$

where (\dots) represents any special arguments inherited from the solutions $\vec{\rho}_0$ and $\vec{\rho}'_0$. In this way, we can find $\vec{z}_{\text{order } 0}(t; (\mathbf{bz}))$ and $\vec{z}'_{\text{order } 0}(t; (\mathbf{bz}))$ from the solutions of Section 5.1, $\vec{z}_{\text{order } 0}(t; (\mathbf{bnz}))$ and $\vec{z}'_{\text{order } 0}(t; (\mathbf{bnz}))$ from the solutions of Section 5.4, $\vec{z}_{\text{order } 0}(t; (\mathbf{bz}), (\mathbf{cw}))$ and $\vec{z}'_{\text{order } 0}(t; (\mathbf{bz}), (\mathbf{cw}))$ from the solutions of Section 6.1, and $\vec{z}_{\text{order } 0}(t; (\mathbf{bnz}), (\mathbf{cw}))$ and $\vec{z}'_{\text{order } 0}(t; (\mathbf{bnz}), (\mathbf{cw}))$ from the solutions of Section 6.4.

Each zeroth-order solution $\vec{z}_{\text{order } 0}$ is the exact solution to the approximation of (7) found via spatial linearization, up to $\mathcal{O}(1)$, under the condition(s) indicated in its special argument(s). In Section 8.2, we discuss the limitations of our spatial linearization approximations.

7.2 Expanded solutions of the original projectile-motion model

In the same way, we find that each expanded position (and its expanded velocity) – and approximate solution of the original, physically motivated system (7) with initial conditions (8) – can be written, for $0 \leq t \leq t_c \tau_\star$, in the form

$$\vec{z}_{\text{expanded}}(t; (\dots)) \equiv \vec{z}_0 + r_c \vec{\rho}_{\text{expanded}} \left(\tau = \frac{t}{t_c}; (\dots) \right), \quad (77a)$$

$$\vec{z}'_{\text{expanded}}(t; (\dots)) \equiv v_c \vec{\rho}'_{\text{expanded}} \left(\tau = \frac{t}{t_c}; (\dots) \right), \quad (77b)$$

where (\dots) represents any special arguments inherited from the solutions $\vec{\rho}_{\text{expanded}}$ and $\vec{\rho}'_{\text{expanded}}$. In this way, we can find $\vec{z}_{\text{expanded}}(t; (\mathbf{bz}))$ and $\vec{z}'_{\text{expanded}}(t; (\mathbf{bz}))$ from the solutions of Section 5.3, $\vec{z}_{\text{expanded}}(t; (\mathbf{bnz}))$ and $\vec{z}'_{\text{expanded}}(t; (\mathbf{bnz}))$ from the solutions of Section 5.6, $\vec{z}_{\text{expanded}}(t; (\mathbf{bz}), (\mathbf{cw}))$ and $\vec{z}'_{\text{expanded}}(t; (\mathbf{bz}), (\mathbf{cw}))$ from the solutions of Section 6.3, and $\vec{z}_{\text{expanded}}(t; (\mathbf{bnz}), (\mathbf{cw}))$ and $\vec{z}'_{\text{expanded}}(t; (\mathbf{bnz}), (\mathbf{cw}))$ from the solutions of Section 6.6.

Each expanded solution $\vec{z}_{\text{expanded}}$ is the exact solution to the approximation of (7) found via spatial linearization, up to $\mathcal{O}(\varepsilon)$, under the condition(s) indicated in its special argument(s). In Section 8.2, we discuss the limitations of our spatial linearization approximations.

8 Model parameters and validity

Here we define the model parameters r_c and t_c introduced in Section 3. We then discuss the temporal region of validity of the perturbation solutions provided in Sections 5 and 6 and in Appendix B.

8.1 Choosing the parameters r_c and t_c

In Section 3, we assumed that we can define values $0 < t_c$ and $0 < r_c$ such that $r_c \ll R_0$ (equivalent to $\varepsilon \ll 1$); the quality of the resulting solutions depends on the assumptions $\eta \ll 1$ and $\varepsilon \ll 1$. In Section 4, we also assumed that we could define r_c such that $\kappa \varepsilon \rho_{\text{max}} \ll 1$; the validity of the spatial expansion of f_{atm} depends on this assumption. For this reason, we need a method to guarantee these conditions.

8.1.1 Bounding r_c based on η

To justify truncating (19), we require that $\eta \ll 1$. To accomplish this, we develop conditions on r_c that guarantee $\eta \leq \eta_{\max}$ for some error-control parameter η_{\max} satisfying

$$0 < \eta_{\max} \ll 1. \quad (78)$$

From (18) and the fact that $\vec{\alpha}$ is a unit vector, we find that

$$\eta = 2\varepsilon(\vec{\alpha} \cdot \vec{\rho}) + \varepsilon^2 \rho^2 \quad (79a)$$

$$\leq 2\varepsilon\rho + \varepsilon^2 \rho^2. \quad (79b)$$

Requiring (79b) $\leq \eta_{\max}$ then implies that

$$\varepsilon\rho \leq \sqrt{1 + \eta_{\max}} - 1. \quad (80)$$

Assuming that there is some parameter ρ_{\max} such that⁴

$$0 < \rho_{\max} \quad \text{and} \quad \rho(\tau) \leq \rho_{\max} \quad \text{for each value of } \tau \text{ at which } \rho \text{ is evaluated,} \quad (81)$$

then the condition (80) is guaranteed if

$$\varepsilon \leq \frac{1}{\rho_{\max}} \left[\sqrt{1 + \eta_{\max}} - 1 \right]; \quad (82)$$

from the definition (17), we then find the requirement that

$$r_c \leq \frac{R_0}{\rho_{\max}} \left[\sqrt{1 + \eta_{\max}} - 1 \right]. \quad (83)$$

As long as η_{\max} satisfies (78) and ρ_{\max} satisfies (81), then any value of r_c satisfying (83) guarantees that $\eta \ll 1$. In this case, our expansion (19k) in terms of η is justified.

8.1.2 Bounding r_c based on ε

To justify our solutions in powers of ε , we require that $\varepsilon \ll 1$, or, equivalently, that $r_c/R_0 \ll 1$. Thus if we want to bound ε by requiring that $\varepsilon \leq \varepsilon_{\max} \exists 0 < \varepsilon_{\max} \ll 1$ chosen as an error-control parameter, then this is guaranteed if $r_c/R_0 \leq \varepsilon_{\max}$, or

$$r_c \leq \varepsilon_{\max} R_0. \quad (84)$$

8.1.3 Bounding r_c based on the spatial expansion of f_{atm}

Looking again at the condition (30),

$$\frac{r_c \rho_{\max}}{\ell} \ll 1, \quad (85)$$

for the spatial expansion of f_{atm} to be valid, we then require that $\text{LHS} \leq \nu_{\max} \exists 0 < \nu_{\max} \ll 1$ chosen as an error-control parameter, or

$$r_c \leq \frac{\ell \nu_{\max}}{\rho_{\max}}. \quad (86)$$

8.1.4 Defining r_c

Putting the conditions (83), (84), and (86) together, we define

$$r_c \equiv \min \left\{ \frac{R_0}{\rho_{\max}} \left[\sqrt{1 + \eta_{\max}} - 1 \right], \varepsilon_{\max} R_0, \frac{\ell \nu_{\max}}{\rho_{\max}} \right\}, \quad (87)$$

where we require only that $0 < \rho_{\max}$, $0 < \eta_{\max} \ll 1$, $0 < \varepsilon_{\max} \ll 1$, and $0 < \nu_{\max} \ll 1$. In Section 11.2 we discuss the choices of the values of these error-control parameters.

⁴See Section 8.2 for a discussion of the parameter ρ_{\max} .

8.1.5 Defining t_c

It would be natural to define the characteristic time t_c to be r_c/v_0 , consistent with [4, p. 2], but we'd like to permit values of the initial speed v_0 that are small, or even zero; instead, we define

$$t_c \equiv \frac{r_c}{\max\{1, v_0\}}. \quad (88)$$

This ensures that t_c is well-defined – both mathematically and numerically – for $0 \leq v_0$, while still providing the intended scaling for many values of v_0 .

8.2 Temporal region of validity of the model and its solutions

The condition (81) requires the value of $\rho(\tau)$ to never exceed the value of the error-control parameter ρ_{\max} . When computing a quantity at dimensionless time τ , then, one must verify that

$$\rho(\tau') \leq \rho_{\max} \quad \forall \tau' \in [0, \tau]. \quad (89)$$

This is because our solutions arise via integrals of the form $\int_0^\tau f(\tau') d\tau'$, which carry the implicit assumption that the integrand is valid at all values of $\tau' \in [0, \tau]$; regions of this closed interval for which $\rho(\tau') > \rho_{\max}$ indicate regions where the condition (81) is violated. In these regions, the condition (83) is suspect, and so the requirement $\eta \ll 1$ is also suspect, putting our expansion in terms of η in jeopardy; in order to guarantee that $\eta \ll 1$ for a particular value of τ , then, one must ensure that (89) holds.

We define the quantity

$$\tau_\star \equiv \max\{\tau \mid (89) \text{ holds}\}; \quad (90)$$

with this definition, the model and subsequent solutions developed in this document are valid for any value of τ satisfying

$$0 \leq \tau \leq \tau_\star. \quad (91)$$

Below are three ways to ensure that the values of τ used for computational purposes satisfy (91).

- (1) One can begin at $\tau = 0$ and increment by some $\Delta\tau$ until the condition (89) is violated.
- (2) One can use a root-finding procedure to determine τ_\star from the condition (89).
- (3) One can bound τ_\star from below by some quantity $\tau_{\max}^{\text{safe}}$, creating an interval $[0, \tau_{\max}^{\text{safe}}]$ within which the solutions can always be safely evaluated.

We focus on strategy (3) and specialize our development to the constant-wind case (**cw**). To find a value $\tau_{\max}^{\text{safe}}$ guaranteed to satisfy

$$0 \leq \tau_{\max}^{\text{safe}} \leq \tau_\star, \quad (92)$$

we consider the speed of the projectile. The projectile's speed can be increased only by the force of gravity or by the force of wind (if the object is at rest or has a tailwind). The magnitude of the acceleration of gravity is bounded above by g , and the magnitude of the acceleration due to a tailwind is bounded above by $\frac{1}{m}b_{\text{drag}}|\vec{v}^{\text{wind}}|$. Defining

$$\hat{g} \equiv g + \frac{1}{m}b_{\text{drag}}|\vec{v}^{\text{wind}}|, \quad (93)$$

we find that the projectile's speed $v = |d\vec{z}/dt|$ satisfies, for $0 \leq t$,

$$v(t) \leq v_{\max}(t) \equiv v_0 + \hat{g}t. \quad (94)$$

We note that equality in (94) is reached exactly when $t = 0$; for $t > 0$, the quantity v_{\max} is the supremum of v across all sets \mathcal{I} of initial conditions and parameters under consideration in this document, representing most closely the case where the projectile begins at rest (so that the force of a tailwind is maximal), very close to the surface of the Earth (so that the acceleration of gravity is well-approximated by g), with wind

in the radially inward direction (so that the forces of gravity and wind directly add). Integrating (94), we find that the projectile's distance $|\vec{r}|$ from its initial position satisfies, for $0 \leq t$,

$$|\vec{r}(t)| \leq r_{\max}(t) \equiv v_0 t + \frac{1}{2} \hat{g} t^2. \quad (95)$$

To find the value of t for which $r_{\max}(t) = r_{\max}^* \ni r_{\max}^* \geq 0$, we solve the quadratic equation

$$\frac{1}{2} \hat{g} t^2 + v_0 t - r_{\max}^* = 0, \quad (96)$$

whose only identically non-negative solution is

$$t_+ \equiv \frac{\sqrt{v_0^2 + 2\hat{g}r_{\max}^*} - v_0}{\hat{g}}. \quad (97)$$

Now, t_+ represents the time required for the projectile to reach the prescribed distance r_{\max}^* from its initial position, in the case where the projectile is moving in a straight line away from its initial position, at its maximum possible speed at every point in time. Thus t_+ is the minimum possible time for the projectile to move the distance r_{\max}^* from its initial position. In other words, t_+ is a tight upper bound for the maximum time for which we can guarantee – across all sets \mathcal{I} of initial conditions and parameters under consideration in this document – that the projectile has moved no farther than r_{\max}^* from its initial position:

$$t_+ = \sup_{\mathcal{I}} \{0 \leq t : |\vec{r}(t)| \leq r_{\max}^*\}. \quad (98)$$

With the condition (89) in mind, we use the relationship (13) to set

$$r_{\max}^* = r_c \rho_{\max}, \quad (99)$$

and we use the relationship (14) to divide t_+ by t_c in order to find the scaled, dimensionless time

$$\tau_{\max}^{\text{safe}} \equiv \frac{\sqrt{v_0^2 + 2\hat{g}r_c\rho_{\max}} - v_0}{t_c \hat{g}}. \quad (100)$$

The quantity $\tau_{\max}^{\text{safe}}$ satisfies the conditions (89), (91), and (92); in fact, $\tau_{\max}^{\text{safe}}$ is the infimum of τ_* across all sets \mathcal{I} of initial conditions and parameters under consideration in this document. The quantity $\tau_{\max}^{\text{safe}}$ plays a crucial role in controlling the error in the computation of trajectories based on our results; see Algorithms 1 and 2 for additional details.

9 Analysis of zeroth-order trajectories with constant wind

Here we discuss in detail the $\mathcal{O}(1)$ solutions subject to the constant-wind condition (**cw**).

9.1 Time of tangency

We now consider the problem of finding the value of τ at which the projectile's motion is tangential to the surface of the Earth.

9.1.1 General condition for the time of tangency

We denote by τ_{tangent} the value of τ satisfying the tangency condition⁵

$$\hat{z}'(t) = 0. \quad (101)$$

To $\mathcal{O}(1)$, the condition (101) is equivalent to

$$\vec{\alpha} \cdot \vec{\rho}' = 0. \quad (102)$$

We note that we can always relate the value of τ_{tangent} to the corresponding value t_{tangent} in the original time scale via the relationship (14).

⁵We could also have used the condition $\vec{z} \cdot \vec{\rho}' = 0$, which produces the same $\mathcal{O}(1)$ condition (102).

9.1.2 Zeroth-order time of tangency for $b_{\text{eff}} = 0$

Using the solution $\vec{\rho}'_0(\tau; (\mathbf{bz}))$ of (37), we find that the $\mathcal{O}(1)$ condition (102) becomes

$$\vec{\alpha} \cdot (\vec{\delta} + \vec{\gamma}\tau) = 0 \quad (103a)$$

$$\delta\sigma + \gamma\tau = 0, \quad (103b)$$

whose solution in the variable τ is

$$\tau_{\text{tangent}}[(\mathbf{bz})] \equiv \frac{\delta\sigma}{|\gamma|}, \quad (104)$$

valid in the interval $[0, \tau_\star]$. Here, the notation $\tau_{\text{tangent}}[(\mathbf{bz})]$ indicates that the quantity τ_{tangent} has inherited the condition (\mathbf{bz}) from the solution $\vec{\rho}'_0(\tau; (\mathbf{bz}))$ used here.

Physical interpretation We point out that the RHS of (104) is the ratio of the component of the initial scaled velocity $\vec{\delta}$ in the initially radially outward direction $\vec{\alpha}$ to the scaled acceleration of strength $|\gamma|$ induced by the zeroth-order force of gravity in the initially radially inward direction $-\vec{\alpha}$. That is, the scaled time $\tau_{\text{tangent}}[(\mathbf{bz})]$ is approximated by the time of ascent of a projectile problem along the $\vec{\alpha}$ -axis, in which the projectile has initial outward speed $\delta\sigma$ and is subjected only to a constant inward gravitational acceleration of magnitude $|\gamma|$. In addition, for the case $b_{\text{eff}} = 0$, the quantity τ_{tangent} is the same as the quantity τ_{ascent} , the time required for the projectile to reach the highest point of its trajectory.

9.1.3 Zeroth-order time of tangency for $b_{\text{eff}} \neq 0$ and constant wind

Using the solution $\vec{\rho}'_0(\tau; (\mathbf{bnz}), (\mathbf{cw}))$ of (64b), we find that the $\mathcal{O}(1)$ condition (102) becomes

$$\vec{\alpha} \cdot (\vec{C} + \vec{D}e^{-\tau/\tau_d}) = 0. \quad (105)$$

Case 1 For $\vec{\alpha} \cdot \vec{C} = 0$, the outward force of wind acting on the projectile when it has no radial motion exactly cancels gravity's inward force, and the condition (105) becomes $\delta\sigma e^{-\tau/\tau_d} = 0$. For $\delta\sigma \neq 0$ there are no solutions: the projectile continues in its initial direction having a non-tangential component, never reaching a point where it is tangential to the surface of the Earth. For $\delta\sigma = 0$, on the other hand, every τ is a solution, as the projectile is, to $\mathcal{O}(1)$, always tangential to the surface of the Earth: when $\delta = 0$, the projectile is suspended in the air, motionless; when $\delta \neq 0$ but $\sigma = 0$, the motion of the projectile is, to $\mathcal{O}(1)$, constrained to lie along the direction of its initial, tangential velocity.

Case 2 If $\vec{\alpha} \cdot \vec{C} \neq 0$ and $\vec{\alpha} \cdot \vec{D} = 0$, then there are no solutions.

Case 3 If $\vec{\alpha} \cdot \vec{C} \neq 0$ and $\vec{\alpha} \cdot \vec{D} \neq 0$, then we find the solution to the $\mathcal{O}(1)$ condition (105) in the variable τ to be

$$\tau_{\text{tangent}}[(\mathbf{bnz}), (\mathbf{cw})] \equiv \tau_d \ln \left(-\frac{\vec{\alpha} \cdot \vec{D}}{\vec{\alpha} \cdot \vec{C}} \right), \quad (106)$$

valid in the interval $[0, \tau_\star]$.

Physical interpretation We observe that the vector $-\vec{D}$ points from the projectile's initial velocity to its asymptotic velocity: $-\vec{D} = \vec{\rho}'_0(\infty; (\mathbf{bnz}), (\mathbf{cw})) - \vec{\rho}'_0(0; (\mathbf{bnz}), (\mathbf{cw}))$. On the other hand, the vector \vec{C} is the asymptotic velocity of the projectile: $\vec{C} = \vec{\rho}'_0(\infty; (\mathbf{bnz}), (\mathbf{cw}))$. Thus the argument of the logarithm of (106) is the ratio of the radially outward component of these two vectors.

9.2 Flight time

We consider the motion of the projectile beginning at the prescribed initial conditions, continuing until the projectile reaches some prescribed final radius R_f satisfying

$$R_f \geq R_E. \quad (107)$$

In cases for which there are both pre-tangent and post-tangent solutions, we provide both solutions.

9.2.1 General condition for the flight time

The flight time can be estimated from the condition

$$R_f = z \quad (108a)$$

$$= R_0 [1 + \varepsilon(\vec{\alpha} \cdot \vec{\rho}_0) + \mathcal{O}(\varepsilon^2)], \quad (108b)$$

where we have used (19l). Taking into account terms up to $\mathcal{O}(1)$, we find the general condition

$$0 = \mu + (\vec{\alpha} \cdot \vec{\rho}_0) \quad (109)$$

for the flight time, where

$$\mu \equiv \frac{R_0 - R_f}{r_c}. \quad (110)$$

We note that μ is a dimensionless length in ρ -space. For this reason, the analyses in the subsections to follow are valid only when

$$|\mu| \leq \rho_{\max}. \quad (111)$$

9.2.2 Zeroth-order flight time for $b_{\text{eff}} = 0$

From the condition (109) and the solution $\vec{\rho}_0(\tau; (\mathbf{bz}))$ of (37), we find the condition

$$0 = \mu + \delta\sigma\tau + \frac{1}{2}\gamma\tau^2, \quad (112)$$

whose solutions are

$$\tau = \frac{\delta\sigma}{|\gamma|} \pm \sqrt{\psi}, \quad (113)$$

where

$$\psi \equiv \frac{\delta^2\sigma^2}{\gamma^2} + \frac{2\mu}{|\gamma|}. \quad (114)$$

In order to select the inward ($z' < 0$) solution corresponding to the later, post-tangent flight time, we define the estimated flight time to be

$$\tau_{\text{flight}}^{\text{post-tan}}[(\mathbf{bz})] \equiv \frac{\delta\sigma}{|\gamma|} + \sqrt{\psi}, \quad (115)$$

valid in the interval $[0, \tau_\star]$. We note that $\tau_{\text{flight}}^{\text{post-tan}}[(\mathbf{bz})]$ is real and non-negative if and only if $\psi \geq 0$; this occurs if and only if $R_f \leq R_{\max}[(\mathbf{bz})]$, where $R_{\max}[(\mathbf{bz})]$ is defined in (128).

We also define the outward ($z' > 0$) solution corresponding to the earlier, pre-tangent flight time to be

$$\tau_{\text{flight}}^{\text{pre-tan}}[(\mathbf{bz})] \equiv \frac{\delta\sigma}{|\gamma|} - \sqrt{\psi}, \quad (116)$$

valid in the interval $[0, \tau_\star]$. We note that $\tau_{\text{flight}}^{\text{pre-tan}}[(\mathbf{bz})]$ is real if and only if $\psi \geq 0$, which occurs if and only if $R_f \leq R_{\max}[(\mathbf{bz})]$. Furthermore, when $\psi \geq 0$, we find that $\tau_{\text{flight}}^{\text{pre-tan}}[(\mathbf{bz})] \geq 0$ if and only if both $\sigma \geq 0$ and $R_0 \leq R_f$.

Physical interpretation We can write the solutions in τ as

$$\tau = \tau_{\text{tangent}}[(\mathbf{bz})] \left(1 \pm \sqrt{1 + \frac{\mu}{\Delta\rho}} \right), \quad (117)$$

where

$$\Delta\rho \equiv \frac{\delta^2 \sigma^2}{2|\gamma|} \quad (118)$$

is the maximum radial displacement of the projectile in ρ -space (see Section 9.3.1).

9.2.3 Zeroth-order flight time for $b_{\text{eff}} \neq 0$ and constant wind

From the condition (109) and the solution $\vec{\rho}_0(\tau; (\mathbf{bnz}), (\mathbf{cw}))$ of (64a), we find that

$$0 = \mu + (\vec{\alpha} \cdot \vec{\rho}_0) \quad (119a)$$

$$= \mu + (\vec{\alpha} \cdot \vec{C})\tau - \tau_d(\vec{\alpha} \cdot \vec{D})(e^{-\tau/\tau_d} - 1) \quad (119b)$$

$$= a_1 + a_2\tau + a_3e^{-\tau/\tau_d}, \quad (119c)$$

where

$$a_2 \equiv (\vec{\alpha} \cdot \vec{C}), \quad (120a)$$

$$a_3 \equiv -\tau_d(\vec{\alpha} \cdot \vec{D}), \quad (120b)$$

$$a_1 \equiv \mu - a_3. \quad (120c)$$

Case 1 If $\vec{\alpha} \cdot \vec{C} = 0$ and $\delta\sigma = 0$, then (119) has a solution if and only if $\mu = 0$, in which case every τ is a solution. In this case, $R_0 = R_f$ and the projectile is initially at radial rest (either $\delta = 0$ and the projectile is at rest, or $\sigma = 0$ and the projectile's motion is initially entirely tangential) with no net radial force, implying that, to $\mathcal{O}(1)$, it remains at radius R_f .

Case 2 If $\vec{\alpha} \cdot \vec{C} = 0$ and $\delta\sigma \neq 0$, then the solution to (119) is given by

$$\tau_{\text{flight}}[\vec{\alpha} \cdot \vec{C} = 0, \delta\sigma \neq 0] = -\tau_d \ln \left(1 + \frac{\mu b_{\text{eff}}}{\delta\sigma} \right). \quad (121)$$

Case 3 If $\vec{\alpha} \cdot \vec{C} \neq 0$ and $\vec{\alpha} \cdot \vec{D} = 0$, then the solution to (119) is given by

$$\tau_{\text{flight}}[\vec{\alpha} \cdot \vec{C} \neq 0, \vec{\alpha} \cdot \vec{D} = 0] = -\frac{\mu}{\vec{\alpha} \cdot \vec{C}}. \quad (122)$$

Case 4 If $\vec{\alpha} \cdot \vec{C} \neq 0$ and $\vec{\alpha} \cdot \vec{D} \neq 0$, then each solution to (119) may be written as

$$\tau = \tau_d W(W_{\text{arg}}) - \frac{a_1}{a_2}, \quad (123)$$

where

$$W_{\text{arg}} \equiv -\frac{a_3 b_{\text{eff}}}{a_2} \exp \left(\frac{a_1 b_{\text{eff}}}{a_2} \right) \quad (124)$$

and where W is the Lambert W function (also called the product log function).

We focus on two branches of the Lambert W function [5], each of which we view as a function $f : \mathbb{R} \rightarrow \mathbb{R}$. The principal branch, denoted W_0 , is an increasing function with domain $[-1/e, \infty)$ and range $[-1, \infty)$; the branch denoted W_{-1} is a decreasing function with domain $[-1/e, 0)$ and range $(-\infty, -1]$. For $-1/e < x < 0$, these branches satisfy $W_{-1}(x) < W_0(x)$, with $W_{-1}(-1/e) = W_0(-1/e) = -1$. We also have that $W_{-1}(xe^x) = x$ for $x \leq -1$ and $W_0(xe^x) = x$ for $x \geq -1$.

Physical interpretation of the branches of the Lambert W function We physically interpret these branches of the multi-valued function W in analogy with the branches of the multi-valued function $\sqrt{\cdot}$. For the function $\sqrt{\cdot}$, we select the branch $+\sqrt{\cdot}$ when we wish to study the later, post-tangent flight time, as in (115), and we select the branch $-\sqrt{\cdot}$ when we wish to study the earlier, pre-tangent flight time, as in (116). The same reasoning can be applied to the function W : one branch characterizes the part of the trajectory occurring before the projectile reaches tangency, while the other branch characterizes the part of the trajectory occurring after the projectile reaches tangency (with the branches converging at the point of tangency, where the trajectory realizes its extreme⁶ radius).

In order to select the post-tangent solution corresponding to the later flight time, we define the estimated flight time to be

$$\tau_{\text{flight}}^{\text{post-tan}}[(\mathbf{bnz}), (\mathbf{cw})] \equiv \tau_d W_0(W_{\text{arg}}) - \frac{a_1}{a_2}, \quad (125)$$

valid in the interval $[0, \tau_\star]$.

We also define the pre-tangent solution corresponding to the earlier flight time as

$$\tau_{\text{flight}}^{\text{pre-tan}}[(\mathbf{bnz}), (\mathbf{cw})] \equiv \tau_d W_{-1}(W_{\text{arg}}) - \frac{a_1}{a_2}, \quad (126)$$

valid in the interval $[0, \tau_\star]$.

9.3 Extreme radii

Here we investigate the extreme values of the radius achieved by the projectile when its trajectory is not interrupted by the Earth and is not terminated by having reached the final radius R_f . In the case (\mathbf{bz}) , this is always a maximum radius; in the case (\mathbf{bnz}) , this can be either a maximum or a minimum radius, the latter possible in the case of wind having a radially outward component – see Figure 1 for schematic representations of some of these cases, and see Figure 3 for a numerical example.

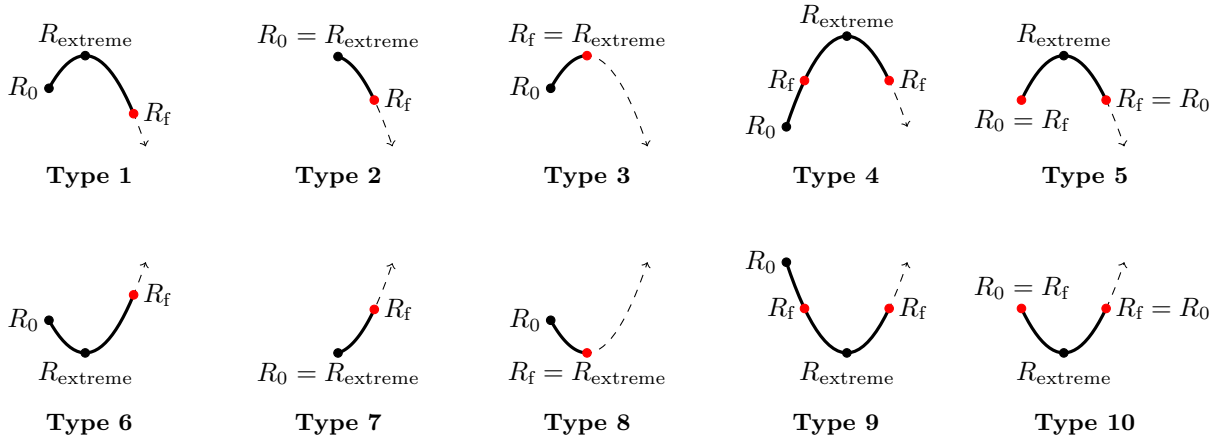


Figure 1: Schematic representations of some possible trajectory types, according to the relative values of R_0 , R_f , and R_{extreme} . Heavy lines are realized trajectories. Dashed arrows indicate the direction of movement. Red dots are solutions to $z = R_f$. See Figures 2 – 6 for numerical examples of some of these trajectory types.

⁶In the case of $b_{\text{eff}} \neq 0$, we discuss *extreme* radii – rather than a *maximum* radius – because the extreme radius can be either a maximum or a minimum (with the help of a radially outward wind force); see Figure 1 for schematic representations of such trajectories, and see Figure 3 for a numerical example of a trajectory reaching an extreme radius that is a minimum.

9.3.1 Maximum radius for $b_{\text{eff}} = 0$

In the case **(bz)**, we found the flight time by choosing the appropriate branch of the multi-valued function $\sqrt{\cdot}$, viewing each branch as a function $f : \mathbb{R} \rightarrow \mathbb{R}$. The branch with greater values corresponded to the later flight time (the inward solution), while the branch with lesser values corresponded to the earlier flight time (the outward solution). Viewing these branches as functions of the desired final radius R_f , these branches converge to a common value when $R_f = R_{\text{max}}$ (that is, when the earlier and later flight times coincide, at the radial peak of the trajectory). For the case **(bz)**, this is when

$$\psi = 0. \quad (127)$$

Solving the condition (127) for R_f and using this value as our approximation of R_{max} , we define

$$R_{\text{max}}[(\mathbf{bz})] \equiv R_0 \left(1 + \varepsilon \frac{\delta^2 \sigma^2}{2|\gamma|} \right), \quad (128)$$

valid when $\tau_{\text{tangent}}[(\mathbf{bz})]$ is valid and when the condition (111) holds. We note that $R_{\text{max}}[(\mathbf{bz})] \geq R_0$.

Physical interpretation We point out the similarity between the fractional term of our result and the maximum height of an elementary projectile in a vacuum: $\delta\sigma$ is the dimensionless initial speed in the radially outward direction, and $|\gamma|$ is the local dimensionless strength of gravity. We also recognize the quantity multiplying ε to be $\Delta\rho$ of (118).

9.3.2 Extreme radius for $b_{\text{eff}} \neq 0$ and constant wind

Following the same argument for the case of non-negligible air resistance and constant wind – but replacing the multi-valued function $\sqrt{\cdot}$ with the multi-valued function W – we find that the earlier and later flight times coincide when

$$W_{\text{arg}} = -\exp(-1). \quad (129)$$

Solving the condition (129) for R_f and using this value as our approximation of R_{extreme} , we define

$$R_{\text{extreme}}[(\mathbf{bnz}), (\mathbf{cw})] \equiv R_0 \left(1 + \varepsilon \tau_d a_2 \left[1 - \frac{a_3 b_{\text{eff}}}{a_2} + \ln \left(\frac{a_3 b_{\text{eff}}}{a_2} \right) \right] \right), \quad (130)$$

valid when $\tau_{\text{tangent}}[(\mathbf{bnz}), (\mathbf{cw})]$ is valid and when the condition (111) holds.

Physical interpretation The quantity multiplying ε in (130) can be written as

$$[\vec{\alpha} \cdot \vec{\rho}'_0(0; (\mathbf{bnz}), (\mathbf{cw}))] \tau_d + [\vec{\alpha} \cdot \vec{\rho}'_0(\infty; (\mathbf{bnz}), (\mathbf{cw}))] \tau_{\text{tangent}}[(\mathbf{bnz}), (\mathbf{cw})]; \quad (131)$$

from this, we see that the initial velocity of the projectile effectively contributes to a change in its radial distance over its time scale of decay, τ_d , and that the asymptotic velocity of the projectile effectively contributes to a change in its radial distance over the entire time scale τ_{tangent} over which the projectile reaches its extreme radius.

9.4 A note on the consistency of our results

As a check on the consistency of our results, each of the following can be shown.

- (1) Pre-tangent and post-tangent flight times both converge to the time of tangency when the condition for branch equality is met:

$$\tau_{\text{flight}}^{\text{pre-tan}}[(\mathbf{bz})] \Big|_{(127)} = \tau_{\text{flight}}^{\text{post-tan}}[(\mathbf{bz})] \Big|_{(127)} = \tau_{\text{tangent}}[(\mathbf{bz})] \quad (132a)$$

and

$$\tau_{\text{flight}}^{\text{pre-tan}}[(\mathbf{bnz}), (\mathbf{cw})] \Big|_{(129)} = \tau_{\text{flight}}^{\text{post-tan}}[(\mathbf{bnz}), (\mathbf{cw})] \Big|_{(129)} = \tau_{\text{tangent}}[(\mathbf{bnz}), (\mathbf{cw})]. \quad (132b)$$

- (2) To $\mathcal{O}(1)$, extreme radii can be found by computing the distance from the projectile to the center of the Earth at the time of tangency:

$$|\vec{z}_0 + r_c \vec{\rho}_0(\tau_{\text{tangent}}[(\mathbf{bz})]; (\mathbf{bz}))| \sim R_{\text{max}}[(\mathbf{bz})] \quad (133a)$$

and

$$|\vec{z}_0 + r_c \vec{\rho}_0(\tau_{\text{tangent}}[(\mathbf{bnz}), (\mathbf{cw})]; (\mathbf{bnz}), (\mathbf{cw}))| \sim R_{\text{extreme}}[(\mathbf{bnz}), (\mathbf{cw})]. \quad (133b)$$

10 Some numerical considerations

Here we discuss some considerations relevant to our numerical implementation of our solutions.

10.1 Estimating the parameter b_{drag}

From [1, p. 44], the linear drag coefficient b_{drag} may be written, in the case of a spherical projectile of diameter D , as

$$b_{\text{drag}} = \zeta_b D, \quad (134)$$

where ζ_b is approximated, in the case of air at standard temperature and pressure, by [1, p. 44]

$$\zeta_b \approx 1.6 \times 10^{-4} \text{ Newtons} \cdot \text{seconds} / \text{meters}^2. \quad (135)$$

We note that the value of ζ_b is dependent upon the properties of the medium: in order to ensure accuracy, one must consider the temperature and pressure of the medium, as well as its fluid characteristics at the speeds over which one wishes to compute projectile motion.

10.2 Small values of b_{eff}

We have provided solutions for both $b_{\text{eff}} = 0$ and $b_{\text{eff}} \neq 0$, but there is a third regime that is important in numerical implementations, where $0 < b_{\text{eff}} \ll 1$. In this regime, $\tau_d \gg 1$. Since the solutions for $b_{\text{eff}} \neq 0$ involve powers of τ_d , these solutions can become numerically unstable. For this reason, in Appendix B, we have provided expanded solutions from the application of a perturbation method with small parameter b_{eff} . This third regime for b_{eff} is taken into account in our numerical implementations of Algorithms 1 and 2; see the Matlab code [6] for complete details.

10.3 Parameterized, error-controlled algorithms

In Section 8.2, we showed that our models would be valid within the time interval $[0, \tau_{\text{max}}^{\text{safe}}]$. When numerically computing a trajectory, then, we restrict our solutions to this time interval; Algorithm 1 provides one method of doing this. If the trajectory has not yet ended – via intersection with either the Earth or with the final radius R_f – by the time $\tau_{\text{max}}^{\text{safe}}$ occurs, then we evaluate the positions and velocities at $\tau_{\text{max}}^{\text{safe}}$ and feed them back into the calculations as the new initial conditions. Algorithm 2 illustrates this process of piecing together subtrajectories to form a complete trajectory and is implemented in the Matlab code [6]. We note that, in our implementation, we ignore any pre-tangent intersection with R_f , choosing to continue the trajectory until either a post-tangent intersection with R_f or an intersection with the Earth. In addition, we have chosen to implement only the constant-wind solutions of Section 6 and Appendix B.

SUBTRAJECTORY		
1	Compute $\tau_{\max}^{\text{safe}}$	See (100)
2	$(\tau_{\text{flight}}^{\text{post-tan}}, \tau_{\text{E}}^{\text{pre-tan}}, \tau_{\text{E}}^{\text{post-tan}}) \leftarrow (\infty, \infty, \infty)$	Initialize
3	Compute μ	See (110)
4	if $ \mu \leq \rho_{\max}$	See (111)
5	Compute $\tau_{\text{flight}}^{\text{post-tan}}$	See (115), (125), and (151)
6	end	
7	Compute $\mu_{\text{E}} \equiv \mu _{R_{\text{f}}=R_{\text{E}}}$	
8	if $ \mu_{\text{E}} \leq \rho_{\max}$	See (111)
9	Compute $\tau_{\text{E}}^{\text{pre-tan}} \equiv \tau_{\text{flight}}^{\text{pre-tan}} _{R_{\text{f}}=R_{\text{E}}}$	See (116), (126), and (151)
10	Compute $\tau_{\text{E}}^{\text{post-tan}} \equiv \tau_{\text{flight}}^{\text{post-tan}} _{R_{\text{f}}=R_{\text{E}}}$	See (115), (125), and (151)
11	end	
12	$\tau_{\text{final}} \leftarrow \min\{\tau_{\max}^{\text{safe}}, \tau_{\text{flight}}^{\text{post-tan}}, \tau_{\text{E}}^{\text{pre-tan}}, \tau_{\text{E}}^{\text{post-tan}}\}$	Effective final scaled time
13	$\text{isLastSubtrajectory} \leftarrow \llbracket \tau_{\text{final}} < \tau_{\max}^{\text{safe}} \rrbracket$	Subtrajectory status
14	Evaluate positions and velocities up to $t_{\text{final}} \equiv t_{\text{c}}\tau_{\text{final}}$	See Sections 7 and B.1
15	return positions, velocities, times, and $\text{isLastSubtrajectory}$	

Algorithm 1: Evaluating a subtrajectory.

We note that Algorithm 2 requires only one evaluation of the vector-valued position and velocity per subtrajectory. Using a root-finding procedure to estimate τ_* (instead of using $\tau_{\max}^{\text{safe}}$, as we have done in Algorithm 1) may result in multiple such function evaluations per subtrajectory, but may also reduce the total number of required subtrajectories. For performance-critical applications, we recommend further study of this trade-off, as we have made no attempt to optimize our numerical implementations of Algorithms 1 and 2.

COMPLETE TRAJECTORY		
1	$\text{isLastSubtrajectory} \leftarrow \text{false}$	Initialize
2	while not $\text{isLastSubtrajectory}$	Loop over subtrajectories
3	Compute subtrajectory and collect outputs	See Algorithm 1
4	Update initial conditions for next subtrajectory	See the code [6]
5	end	
6	return collected positions, velocities, and times	

Algorithm 2: Evaluating a complete trajectory.

11 Numerical results

Here we present some numerical results. All of our results were produced from the Matlab code [6], which we have made freely available on Matlab File Exchange. The code therein implements Algorithms 1 and 2, outputs figures in the Matlab Live Script `lpd_demo.mlx`, and saves the data in the `.csv` files that we used in generating Figures 2 – 6 of this document.

11.1 Quantities of interest

We define the following quantities. Here, t_i is the i^{th} time step, with $0 \leq i$ and $t_0 = 0$. Quantities computed via our implementation of the methods of this document are denoted by $(\cdot)_{\text{ours}}$, and quantities computed via Matlab’s numerical ODE solver are denoted by $(\cdot)_{\text{num}}$.

- The relative error in the satisfaction of the ODE (7) is defined by the difference between the vector-valued LHS and vector-valued RHS of the original model (7), divided by⁷ its RHS:

$$E_{\text{ODE}}(t_i) \equiv \frac{|(\vec{7})_{\text{LHS}}(t_i) - (\vec{7})_{\text{RHS}}(t_i)|}{|(\vec{7})_{\text{RHS}}(t_i)|}. \quad (136)$$

- The deviation in position is defined by

$$\Delta_{\vec{z}}(t_i) \equiv |\vec{z}_{\text{ours}}(t_i) - \vec{z}_{\text{num}}(t_i)|, \quad (137)$$

having units of meters.

- The deviation in velocity is defined by

$$\Delta_{\vec{z}'}(t_i) \equiv |\vec{z}'_{\text{ours}}(t_i) - \vec{z}'_{\text{num}}(t_i)|, \quad (138)$$

having units of meters / second.

We call special attention to the fact that E_{ODE} is the key metric quantifying the performance of each method. This is because each method is designed to approximately solve the original ODE (7). In particular, the expanded solutions we provide are designed to improve the accuracy of the zeroth-order solutions *with respect to the original ODE* (7). This is *not* necessarily the same thing as improving the accuracy of the zeroth-order positions or velocities. Indeed, in Figure 5, we provide an example for which the expanded and numerical positions have the lowest values of E_{ODE} , whereas the zeroth-order and numerical positions are closer to one another. Thus we focus on position and velocity *deviations* from the numerical solutions – rather than *errors* – because there is no guarantee that the numerical solutions more accurately compute the position and velocity than our solutions do, even in cases where the numerical solution achieves a lower value of E_{ODE} .

11.2 Trajectory comparisons

Below we present comparisons of trajectories and related quantities defined in Section 11.1, computed both via the methods of this document and via Matlab’s `ode15s` stiff ODE solver [7], with absolute and relative tolerances set to $5\text{e-}14$.

All trajectories we present have the following in common.

- We have set the atmospheric thinning function to be $f_{\text{atm}}(s) = e^{-s}$, with characteristic length scale $\ell = 10,000$ meters.
- We have set the value of the parameter b_{eff}^* to be $b_{\text{eff}}^* = 1\text{e-}6$ (empirically determined); see Appendix B for more information about the parameter b_{eff}^* .
- We have set the value of the parameter ρ_{max} to be $\rho_{\text{max}} = 1$.
- In addition, the values of the error-control parameters ε_{max} , ν_{max} , and η_{max} were always set to be equal to one another; we call the common value of these error-control parameters e_{max} , and we vary

⁷We have chosen the RHS – as opposed to the LHS – as the denominator for no particular reason.

e_{\max} – and thus simultaneously vary ε_{\max} , ν_{\max} , and η_{\max} together – in the experiments to follow.⁸

Table 1 outlines some of the inputs used in producing Figures 2 – 6. We have tried to explore a reasonable variety of input parameter ranges and trajectory types⁹ without providing an overwhelming number of examples. Details of the size¹⁰ and mass of each projectile can be found in our numerical implementation [6].

Figure	Object	e_{\max}	R_0	v_0	θ_r	ϕ_r	θ_v	ϕ_v	\vec{v}^{wind}	R_f
2	point mass	1e-3	R_E	1e4	$\frac{1}{3}$	$\frac{1}{2}$	$\frac{1}{10}$	$\frac{1}{2}$		$1.2R_E$
3	raindrop	1e-3	$R_E + 100$	50			1		(0, 0, 5e5)	$R_E + 80$
4	golf ball	5e-3	R_E	70			$\frac{1}{3}$	$\frac{1}{2}$	(-10, 10, 2)	R_E
5	baseball	1e-2	R_E	30		$\frac{1}{2}$	$\frac{1}{4}$	$\frac{1}{2}$		R_E
6	beach ball	5e-4	$1.1R_E$						(100, -100, -100)	$1.05R_E$

Table 1: Inputs for Figures 2 – 6. Omitted values are zeros. Units are as follows: e_{\max} (dimensionless); R_0 and R_f (meters); v_0 and \vec{v}^{wind} (meters / second); θ_r , ϕ_r , θ_v , and ϕ_v (π radians).

In Figures 2 – 6, the time t along each horizontal axis is expressed in units of seconds. The radial trajectories show the distance z of the projectile from the center of the Earth, minus R_E , expressed in units of meters.

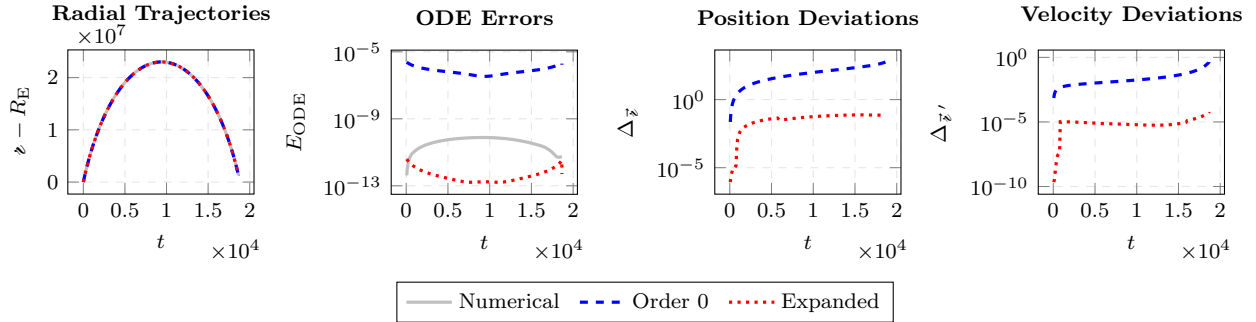


Figure 2: Data for a point mass (generated with inputs from Table 1). Since a point mass has size zero, it experiences no air resistance; as an additional quality check, the total energy of the projectile at the end of its trajectory is conserved to within the following fraction of the total energy of the projectile at the start of its trajectory: Numerical (6.0e-13), Order 0 (9.0e-7), Expanded (1.6e-11). This trajectory is an example of trajectory Type 4 of Figure 1.

⁸We have found empirically that the best accuracy is achieved when $e_{\max} \in [5e-4, 1e-1]$, with smaller values generally resulting in better accuracy but more computational time.

⁹See the captions of Figures 2 – 6 for how each trajectory corresponds to a specific trajectory type from Figure 1.

¹⁰The size of the projectile is used in estimating the parameter b_{drag} , as in Section 10.1.

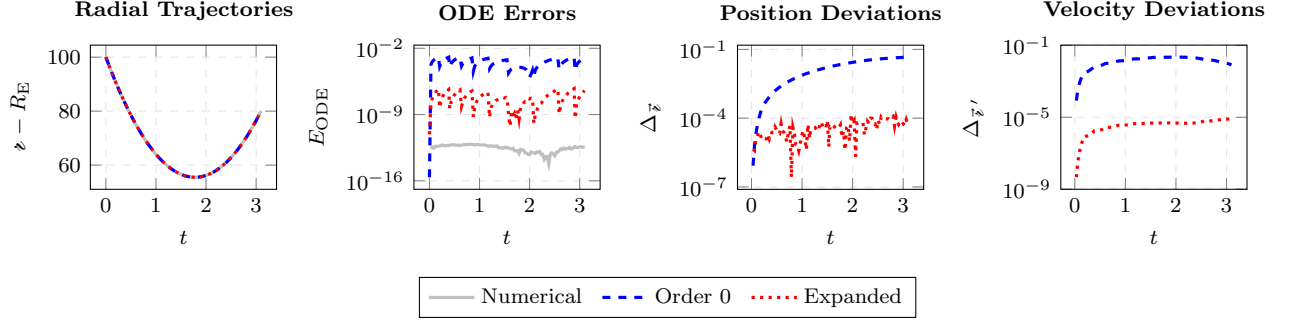


Figure 3: Data for a raindrop (generated with inputs from Table 1). Note that this trajectory achieves a minimum radius above the surface of the Earth (without being interrupted by R_f), providing an example of trajectory Type 9 of Figure 1.

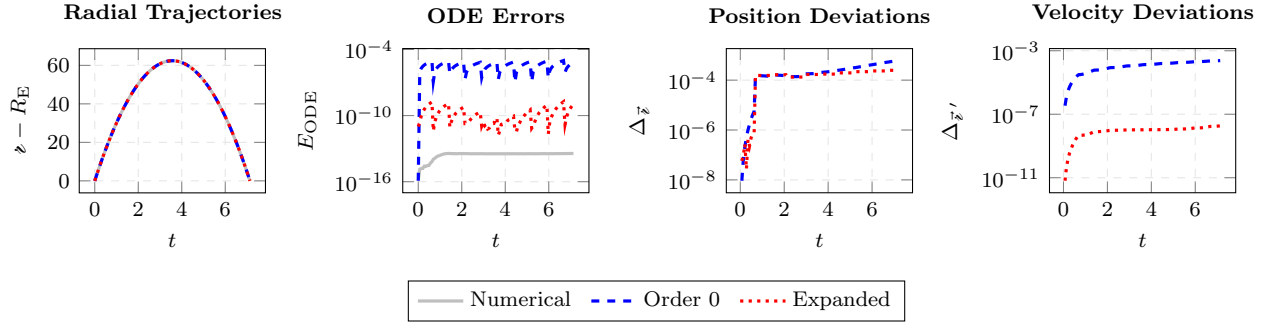


Figure 4: Data for a golf ball (generated with inputs from Table 1). This trajectory is an example of trajectory Type 5 of Figure 1.

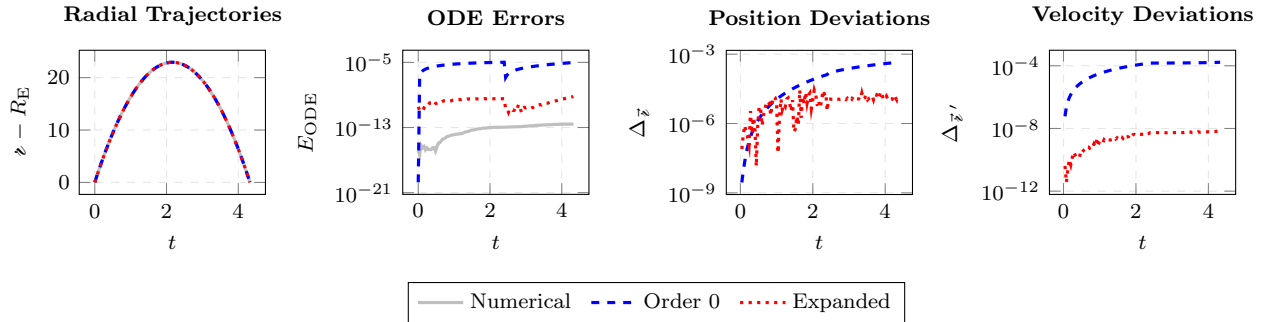


Figure 5: Data for a baseball (generated with inputs from Table 1). Note that, for $0 < t \lesssim 0.5$, we have that $(E_{ODE})_{\text{Numerical}} \ll (E_{ODE})_{\text{Expanded}} \ll (E_{ODE})_{\text{Order 0}}$ and yet $(\Delta_z)_{\text{Order 0}} \ll (\Delta_z)_{\text{Expanded}}$. In other words, the Expanded and Numerical positions most closely satisfy the ODE (7) but are not closest to one another, pair-wise. This trajectory is an example of trajectory Type 5 of Figure 1.

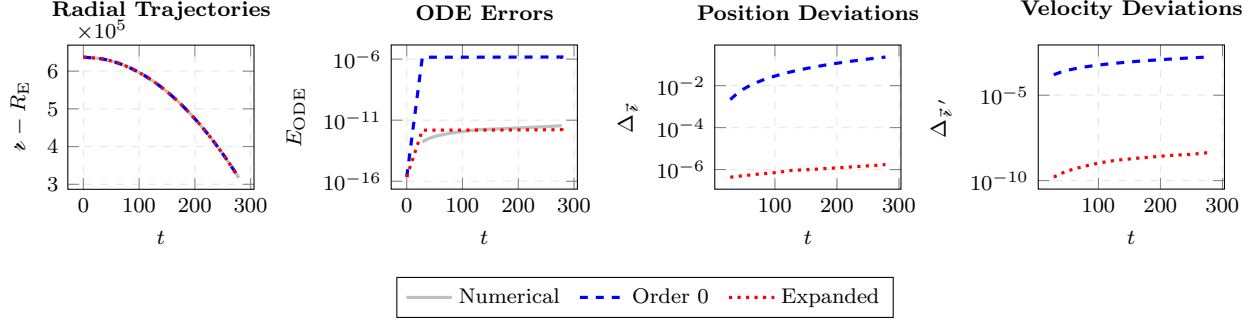


Figure 6: Data for a beach ball (generated with inputs from Table 1). This trajectory is an example of trajectory Type 1 of Figure 1.

11.3 Some observations

We make the following observations of Figures 2 – 6.

- (1) In each figure, we observe that $(E_{\text{ODE}})_{\text{Expanded}} \ll (E_{\text{ODE}})_{\text{Order 0}}$, providing numerical evidence that our $\mathcal{O}(\varepsilon)$ solutions improve upon our $\mathcal{O}(1)$ solutions, in the sense that they reduce the error in the original ODE (7).
- (2) In Figure 2, we see that $(E_{\text{ODE}})_{\text{Expanded}} \ll (E_{\text{ODE}})_{\text{Numerical}}$, providing numerical evidence that our expanded solutions can be highly accurate with respect to the original ODE (7), depending on the particular problem and on the chosen values of the error-control parameters.

12 Conclusion

In this paper, we provided a full 3D treatment of the classic linear projectile problem, subject to several generalizations. By applying a perturbation technique with small parameter ε , we provided exact integral solutions to $\mathcal{O}(\varepsilon)$ for the general problem and exact closed-form solutions to $\mathcal{O}(\varepsilon)$ for the special case of constant wind. We investigated the time of tangency, times of flight, and extreme values of the radius achieved by the projectile. We developed a method to control the error in our approximations and provided algorithms utilizing this method. We then provided numerical evidence that our $\mathcal{O}(\varepsilon)$ solutions increase the accuracy of our $\mathcal{O}(1)$ solutions with respect to the ODE modeling the physical problem. We have also made freely available our Matlab code that reproduces all the numerical data presented in this paper.

A Selected calculations of the integrals I_0 and I_1

We find, for $b_{\text{eff}} \neq 0$, that

$$I_0[x \mapsto 1](\tau) = \int_0^\tau e^{\tau'/\tau_d} d\tau' \quad (139a)$$

$$= \tau_d(e^{\tau/\tau_d} - 1), \quad (139b)$$

$$e^{-\tau/\tau_d} I_0[x \mapsto 1](\tau) = \tau_d(1 - e^{-\tau/\tau_d}), \quad (139c)$$

$$I_1[x \mapsto 1](\tau) = \int_0^\tau e^{-\tau'/\tau_d} I_0[x \mapsto 1](\tau') d\tau' \quad (139d)$$

$$= \tau_d \int_0^\tau (1 - e^{-\tau'/\tau_d}) d\tau' \quad (139e)$$

$$= \tau_d^2(e^{-\tau/\tau_d} - 1) + \tau_d\tau, \quad (139f)$$

$$I_0[x \mapsto x](\tau) = \int_0^\tau e^{\tau'/\tau_d} \tau' d\tau' \quad (140a)$$

$$= \tau_d^2(1 - e^{-\tau/\tau_d}) + \tau_d \tau e^{-\tau/\tau_d}, \quad (140b)$$

$$e^{-\tau/\tau_d} I_0[x \mapsto x](\tau) = \tau_d^2(e^{-\tau/\tau_d} - 1) + \tau_d \tau, \quad (140c)$$

$$I_1[x \mapsto x](\tau) = \int_0^\tau e^{-\tau'/\tau_d} I_0[x \mapsto x](\tau') d\tau' \quad (140d)$$

$$= \int_0^\tau \tau_d^2(e^{-\tau'/\tau_d} - 1) + \tau_d \tau' d\tau' \quad (140e)$$

$$= \tau_d \tau (\frac{1}{2} \tau - \tau_d) + \tau_d^3(1 - e^{-\tau/\tau_d}), \quad (140f)$$

$$I_0[x \mapsto e^{-x/\tau_d}](\tau) = \int_0^\tau d\tau' \quad (141a)$$

$$= \tau, \quad (141b)$$

$$e^{-\tau/\tau_d} I_0[x \mapsto e^{-x/\tau_d}](\tau) = \tau e^{-\tau/\tau_d}, \quad (141c)$$

$$I_1[x \mapsto e^{-x/\tau_d}](\tau) = \int_0^\tau e^{-\tau'/\tau_d} I_0[x \mapsto e^{-x/\tau_d}](\tau') d\tau' \quad (141d)$$

$$= \int_0^\tau e^{-\tau'/\tau_d} \tau' d\tau' \quad (141e)$$

$$= \tau_d^2(1 - e^{-\tau/\tau_d}) - \tau_d \tau e^{-\tau/\tau_d}, \quad (141f)$$

$$I_0[x \mapsto x e^{-x/\tau_d}](\tau) = \int_0^\tau \tau' d\tau' \quad (142a)$$

$$= \frac{1}{2} \tau^2, \quad (142b)$$

$$e^{-\tau/\tau_d} I_0[x \mapsto x e^{-x/\tau_d}](\tau) = \frac{1}{2} \tau^2 e^{-\tau/\tau_d}, \quad (142c)$$

$$I_1[x \mapsto x e^{-x/\tau_d}](\tau) = \int_0^\tau e^{-\tau'/\tau_d} I_0[x \mapsto x e^{-x/\tau_d}](\tau') d\tau' \quad (142d)$$

$$= \frac{1}{2} \int_0^\tau e^{-\tau'/\tau_d} (\tau')^2 d\tau' \quad (142e)$$

$$= \tau_d^3(1 - e^{-\tau/\tau_d}) - e^{-\tau/\tau_d} \tau_d \tau (\tau_d + \frac{1}{2} \tau), \quad (142f)$$

$$I_0[x \mapsto e^{-2x/\tau_d}](\tau) = \int_0^\tau e^{-\tau'/\tau_d} d\tau' \quad (143a)$$

$$= \tau_d(1 - e^{-\tau/\tau_d}), \quad (143b)$$

$$e^{-\tau/\tau_d} I_0[x \mapsto e^{-2x/\tau_d}](\tau) = \tau_d e^{-\tau/\tau_d} (1 - e^{-\tau/\tau_d}), \quad (143c)$$

$$I_1[x \mapsto e^{-2x/\tau_d}](\tau) = \int_0^\tau e^{-\tau'/\tau_d} I_0[x \mapsto e^{-2x/\tau_d}](\tau') d\tau' \quad (143d)$$

$$= \tau_d \int_0^\tau e^{-\tau'/\tau_d} (1 - e^{-\tau'/\tau_d}) d\tau' \quad (143e)$$

$$= \frac{1}{2} \tau_d^2 (e^{-\tau/\tau_d} - 1)^2. \quad (143f)$$

B Expansions in orders of b_{eff}

Here we effectively apply a perturbation technique using the quantity b_{eff} , which we assume to be small. More specifically, we assume that the condition

$$b_{\text{eff}} < b_{\text{eff}}^* \quad (\text{bs})$$

holds for some appropriately chosen¹¹ parameter $b_{\text{eff}}^* \ll 1$.

B.1 Expanded positions and velocities

We write the Ansatz

$$\vec{\rho}_0(\tau; (\mathbf{bs}), (\mathbf{cw})) = \vec{\rho}_0^{(0)}(\tau; (\mathbf{bs}), (\mathbf{cw})) + b_{\text{eff}} \vec{\rho}_0^{(1)}(\tau; (\mathbf{bs}), (\mathbf{cw})) + \mathcal{O}(b_{\text{eff}}^2), \quad (144)$$

where the components $\vec{\rho}_0^{(j)}$ are to be determined. To find these components, we can equivalently (1) Taylor-expand the general solution $\vec{\rho}_0(\tau; (\mathbf{bnz}), (\mathbf{cw}))$ in powers of b_{eff} or (2) re-cast the IVP for $\vec{\rho}_0(\tau; (\mathbf{bnz}), (\mathbf{cw}))$ into one IVP for each order of b_{eff} in which we're interested.

We find that

$$\vec{\rho}_0^{(0)}(\tau; (\mathbf{bs}), (\mathbf{cw})) = \vec{\rho}_0(\tau; (\mathbf{bz}), (\mathbf{cw})), \quad (145a)$$

$$(\vec{\rho}_0^{(0)})'(\tau; (\mathbf{bs}), (\mathbf{cw})) = \vec{\rho}_0'(\tau; (\mathbf{bz}), (\mathbf{cw})), \quad (145b)$$

$$\vec{\rho}_0^{(1)}(\tau; (\mathbf{bs}), (\mathbf{cw})) = \frac{1}{2}(\vec{w}_0 - \vec{\delta})\tau^2 - \frac{1}{6}\vec{\gamma}\tau^3, \quad (145c)$$

$$(\vec{\rho}_0^{(1)})'(\tau; (\mathbf{bs}), (\mathbf{cw})) = (\vec{w}_0 - \vec{\delta})\tau - \frac{1}{2}\vec{\gamma}\tau^2. \quad (145d)$$

The zeroth-order solutions to the original problem (7) are defined in the usual way, for $0 \leq t \leq t_c \tau_*$:

$$\vec{z}_{\text{order } 0}(t; (\mathbf{bs}), (\mathbf{cw})) \equiv \vec{z}_0 + r_c \vec{\rho}_0 \left(\tau = \frac{t}{t_c}; (\mathbf{bs}), (\mathbf{cw}) \right), \quad (146a)$$

$$\vec{z}'_{\text{order } 0}(t; (\mathbf{bs}), (\mathbf{cw})) \equiv v_c \vec{\rho}_0' \left(\tau = \frac{t}{t_c}; (\mathbf{bs}), (\mathbf{cw}) \right). \quad (146b)$$

Applying the same technique, we find the components of $\vec{\rho}_1(\tau; (\mathbf{bs}), (\mathbf{cw}))$ to be given by

$$\vec{\rho}_1^{(0)}(\tau; (\mathbf{bs}), (\mathbf{cw})) = \vec{\rho}_1(\tau; (\mathbf{bz}), (\mathbf{cw})), \quad (147a)$$

$$(\vec{\rho}_1^{(0)})'(\tau; (\mathbf{bs}), (\mathbf{cw})) = \vec{\rho}_1'(\tau; (\mathbf{bz}), (\mathbf{cw})), \quad (147b)$$

$$\vec{\rho}_1^{(1)}(\tau; (\mathbf{bs}), (\mathbf{cw})) = -2\vec{p}_1(e^{-\tau} - 1) - 2\vec{p}_1\tau + \vec{p}_1\tau^2 - \frac{1}{3}\vec{p}_1\tau^3 + (\frac{1}{4}\vec{p}_3 - \vec{p}_4)\tau^4 + \frac{1}{5}\vec{p}_4\tau^5, \quad (147c)$$

$$(\vec{\rho}_1^{(1)})'(\tau; (\mathbf{bs}), (\mathbf{cw})) = 2\vec{p}_1(e^{-\tau} - 1) + 2\vec{p}_1\tau - \vec{p}_1\tau^2 + 4(\frac{1}{4}\vec{p}_3 - \vec{p}_4)\tau^3 + \vec{p}_4\tau^4, \quad (147d)$$

where

$$\vec{p}_2 \equiv -\frac{1}{2}\gamma(\vec{\delta} - \vec{w}_0) + \frac{3}{2}\vec{\gamma}(\delta\sigma - \vec{\alpha} \cdot \vec{w}_0) + \frac{1}{2}(3\delta\sigma - \vec{\alpha} \cdot \vec{w}_0)(\vec{\delta} - \vec{w}_0)b'_{\text{eff}}, \quad (148a)$$

$$\vec{p}_3 \equiv \frac{1}{3}\gamma\vec{\gamma} + \frac{2}{3}b'_{\text{eff}}\gamma(\vec{\delta} - \vec{w}_0) + b'_{\text{eff}}\vec{\gamma}(\delta\sigma - \frac{1}{2}\vec{\alpha} \cdot \vec{w}_0), \quad (148b)$$

$$\vec{p}_4 \equiv \frac{5}{12}\gamma\vec{\gamma}b'_{\text{eff}}, \quad (148c)$$

$$\vec{p}_1 \equiv -\vec{p}_2 + 3\vec{p}_3 - 12\vec{p}_4. \quad (148d)$$

Neglecting terms of order b_{eff}^2 and higher, we then write the (doubly) expanded dimensionless position, for $0 \leq \tau \leq \tau_*$, as

$$\vec{\rho}_{\text{expanded}}(\tau; (\mathbf{bs}), (\mathbf{cw})) \equiv \vec{\rho}_0(\tau; (\mathbf{bs}), (\mathbf{cw})) + \varepsilon \vec{\rho}_1(\tau; (\mathbf{bs}), (\mathbf{cw})) \quad (149a)$$

$$\begin{aligned} &= \left[\vec{\rho}_0^{(0)}(\tau; (\mathbf{bs}), (\mathbf{cw})) + b_{\text{eff}} \vec{\rho}_0^{(1)}(\tau; (\mathbf{bs}), (\mathbf{cw})) \right] \\ &\quad + \varepsilon \left[\vec{\rho}_1^{(0)}(\tau; (\mathbf{bs}), (\mathbf{cw})) + b_{\text{eff}} \vec{\rho}_1^{(1)}(\tau; (\mathbf{bs}), (\mathbf{cw})) \right], \end{aligned} \quad (149b)$$

¹¹See Section 11.2 for an example value of b_{eff}^* .

with the (doubly) expanded dimensionless velocity $\vec{\rho}'_{\text{expanded}}$ defined similarly. The (doubly) expanded position $\vec{z}_{\text{expanded}}$ and velocity $\vec{z}'_{\text{expanded}}$ are then defined accordingly, for $0 \leq t \leq t_c \tau_*$:

$$\vec{z}_{\text{expanded}}(t; (\mathbf{bs}), (\mathbf{cw})) \equiv \vec{z}_0 + r_c \vec{\rho}_{\text{expanded}} \left(\tau = \frac{t}{t_c}; (\mathbf{bs}), (\mathbf{cw}) \right), \quad (150a)$$

$$\vec{z}'_{\text{expanded}}(t; (\mathbf{bs}), (\mathbf{cw})) \equiv v_c \vec{\rho}'_{\text{expanded}} \left(\tau = \frac{t}{t_c}; (\mathbf{bs}), (\mathbf{cw}) \right). \quad (150b)$$

B.2 Expanded times of tangency and flight

Using Ansatzes of the same form as (144), we find that

$$(\tau_{\text{tangent}}[(\mathbf{bs}), (\mathbf{cw})])^{(0)} = \tau_{\text{tangent}}[(\mathbf{bz})], \quad (151a)$$

$$(\tau_{\text{tangent}}[(\mathbf{bs}), (\mathbf{cw})])^{(1)} = \frac{2}{\gamma}(\vec{\alpha} \cdot \vec{w}_0 - \delta\sigma), \quad (151b)$$

$$(\tau_{\text{flight}}^{\text{post-tan}}[(\mathbf{bs}), (\mathbf{cw})])^{(0)} = \tau_{\text{flight}}^{\text{post-tan}}[(\mathbf{bz}), (\mathbf{cw})], \quad (151c)$$

$$(\tau_{\text{flight}}^{\text{post-tan}}[(\mathbf{bs}), (\mathbf{cw})])^{(1)} = \frac{3}{\gamma}(\vec{\alpha} \cdot \vec{w}_0 - \delta\sigma), \quad (151d)$$

$$(\tau_{\text{flight}}^{\text{pre-tan}}[(\mathbf{bs}), (\mathbf{cw})])^{(0)} = \tau_{\text{flight}}^{\text{pre-tan}}[(\mathbf{bz}), (\mathbf{cw})], \quad (151e)$$

$$(\tau_{\text{flight}}^{\text{pre-tan}}[(\mathbf{bs}), (\mathbf{cw})])^{(1)} = \frac{3}{\gamma}(\vec{\alpha} \cdot \vec{w}_0 - \delta\sigma). \quad (151f)$$

References

- [1] J. Taylor, “Classical Mechanics”, University Science Books, 2005.
- [2] R. Bernardo, J. Esguerra, J. Valleyos, and J. Canda, “Wind-influenced projectile motion”, *Eur. J. Phys.* **36** (2015).
- [3] M. Lubarda and V. Lubarda, “A review of the analysis of wind-influenced projectile motion in the presence of linear and nonlinear drag force”, *Archive of Applied Mathematics* (2022) **92**:1997–2017.
- [4] M. Holmes, “Introduction to Perturbation Methods”, Second Edition, Springer, 2013.
- [5] R. Roy and F. Olver, *Lambert W Function* in F. Olver, D. Lozier, R. Boisvert, and C. Clark (eds.), “NIST Handbook of Mathematical Functions”, Cambridge University Press, 2010.
- [6] N. Lorenzo, “Computing Trajectories of a More General Linear Projectile”, Matlab File Exchange, <https://www.mathworks.com/matlabcentral/fileexchange/174950-computing-trajectories-of-a-more-general-linear-projectile>.
- [7] *Matlab Documentation*, <https://www.mathworks.com/help/matlab/ref/ode15s.html>, accessed 24 Oct 2024.